Report on the Ore Mineralogy of Samples from the Au-Rich 1806 Zone, Ming Volcanogenic Massive Sulfide (VMS) Deposit, Baie Verte, Newfoundland

Prepared For:
Rambler Metals and Mining
C/O Larry Pilgrim, BSc, PGeo
Chief Geologist
P.O. Box 291, Baie Verte, NL, A0K 1B0
Phone: (709) 532 4990
Fax: (709) 532 4992
Cell: (709) 532 7111
E-mail: lpilgrim@ramblermines.com

Prepared by:
Stephen J. Piercey, PhD, PGeo
Stephen J. Piercey Geological Consulting
11 First Avenue
St. John's, NL
A1B 1N3
Ph. 709.579.9099
Fax. 709.737.7437
Email: spiercey@sjpgeoconsulting.com
Web: www.sjpgeoconsulting.com

Preliminary Draft: Saturday, January 17, 2009

Executive Summary

The 1806 Zone of the Ming VMS deposit is a base- and precious-metal-enriched sulfide zone with Au-Ag-enrichment similar to many world-class Au-rich VMS systems. The ore mineralogy of the deposit is dominated by various sulfide, sulfosalt, native metal, and oxide phases. Sulfides are variably recrystallized due to deformation and metamorphism and are strongly recrystallized and contact metamorphosed in proximity to younger mafic dykes. Massive sulfide distal from dyke margins, despite being deformed and recrystallized, are likely representative of the primary VMS-bearing assemblage given typical VMS-related mineral assemblages that dominates the sulfides (e.g., pyrite-chalcopyrite-sphalerite-galena). These massive sulfides are dominated by variable amounts of sulfide (pyrite, chalcopyrite, sphalerite, galena, and arsenopyrite), sulfosalts (tetrahedrite, boulangerite, stannite, mawsonite, tennantite), and Au (electrum?). Massive sulfide that has been recrystallized and contact metamorphism in proximity to mafic dykes are characterized by buckshot textures with abundant pyrrhotite-rich sulfides with pyrite porphyroblasts, and lesser sphalerite, chalcopyrite, galena, sulfosalts, and magnetite. Notably, these buckshot ore samples are rich in iridescent bismuthinite and have a very minor amount of arsenopyrite, much lower than in the primary VMS-bearing sulfides.

Gold show four main associations in the 1806 Zone: 1) in association with atoll-like intergrowths of chalcopyrite, tetrahedrite, and arsenopyrite with or without sphalerite; 2) within and along the edges of tetrahedrite grains; 3)spatially associated with arsenopyrite porphyryblasts and tetrahedrite, chalcopyrite, and boulangerite; and 4) between grains of pyrite and arsenopyrite either by itself or intergrown with boulangerite or bismuthinite. In all cases Au is spatially associated with arsenopyrite and sulfosalt phases. In the fourth case, however, Au is associated with structural void space in between annealed arsenopyrite and pyrite crystals. In all cases gold is spatially associated with grain margins and not in the cores of mineral grains, suggesting the potential for liberation; further testing of milled concentrates is required to prove this hypothesis. While deformation has played a role in remobilizing and potentially liberating Au (e.g., type 4 gold above), the strong association with arsenopyrite, Sb-As-rich sulfosalts, and magmatic element enrichments in assays (e.g., anomalous Cu-Sb-As-Hg-Ag) suggest that the Au was introduced by magmatic fluids and was not the product of an orogenic overprint as has been suggested by some other workers. The geological, mineralogical, and chemical attributes of the massive sulfides from the 1806 Zone are similar to other Au-Ag-rich VMS systems globally (e.g., Bousquet-LaRonde; Eskay Creek; Boliden; Mount Lyell), but the geological setting, ore mineralogy, and deformation style is most similar to the deposits of the Bousquet-LaRonde district in Quebec.

It is recommended that further microanalytical work (e.g., SEM, electron microprobe, mineral liberation analysis) be performed on these samples to further constrain the mineralogy, residence of precious metals and base metals, and the location and residence of potential deleterious elements. A concentrate study that complements this study is imperative to better understand the liberation of various phases in this deposit. Longer term, there is much potential to continue research into comparisons of the setting and

massive sulfide mineralogy of different zones in the Ming deposit, their alteration envelopes, and to better understand the base, precious, and trace metal zoning within the 1806 and other zones in the Ming VMS system using the existing assay database.

Introduction

The 1806 Zone of the Ming volcanogenic massive sulfide (VMS) deposit represents an unusually Au-rich VMS lens in comparison to average VMS deposits. The deposit is hosted by a bimodal assemblage of strongly deformed Ordovician mafic and felsic volcanic and volcaniclastic rocks that are cross-cut by mafic dykes. The 1806 Zone is hosted at the contact between footwall felsic volcanic and volcaniclastic rocks and hanging wall mafic volcaniclastic and sedimentary rocks. In many cases the sulfides are cut by late, coarse- to medium-grained mafic dykes. In this report, the ore mineralogy of massive sulfides from this Au-rich lens are examined to determine the sulfide mineralogy and the residence and location of Au within the 1806 Zone. These data provide important insights into the genesis of the 1806 Zone and provide the fodder for comparisons to other Au-rich VMS systems globally.

Samples and Methodology

Samples for thin section petrography were taken from drill holes in the Au-rich 1806 zone of the Ming VMS deposit. Samples were taken from holes RMUG08-120, 123, 125, 139 and 142. These holes were chosen as they contained representative types of sulfide mineralization styles and mineral assemblages. Samples were taken of all representative mineralization types (e.g., sphalerite-rich, tetrahedrite-rich, arsenopyrite-rich, Au-rich, metamorphosed buckshote ore, etc), and those that had high Au assays. A standard reflected light petrographic microscope was utilized for observing thin sections. Each thin section contains photos that are indexed to the sample number, and each section contains a digital collage of representative photos and assemblages for a given sample; the latter collages are figures in this report. All digital images taken, regardless of quality, and all files are provided to Rambler Metals and Mining in digital form. Appendix A contains a summary table of minerals present in the various sections and assays for the intersections that contain these sections. There is often a good correlation between sulfide mineralogy and the assay grades. In this table, however, there is some discrepancy between Au grades and presence of Au. This is likely due to the nuggety nature of Au and the size of the samples (e.g., typically 5cm or less) – it does not necessarily mean there is no visible gold present in the sulfide assemblage over the assay interval, especially given the presence of visible gold in many samples within the 1806 Zone; however, this is a possibility.

Thin Section Results

Sulfide minerals within the 1806 zone include sulfides, sulfosalts, oxides and native metals (Table 1). The predominant sulfide mineral phases include pyrite, chalcopyrite, arsenopyrite, sphalerite, and galena, with lesser pyrrhotite, bismuthinite, covellite, and chalcocite. The sulfosalt phases are dominated by tetrahedrite, which is an essential mineral in many samples, and lesser tennantite, boulangerite, stannite, and mawsonite. Magnetite is present with pyrrhotite in the recrystallized buckshot sulfides that occur

proximal to mafic dykes; both these phase are restricted to dyke-proximal sulfides. Gold is present in native form, commonly associated with sulfosalts, chalcopyrite, pyrite and arsenopyrite. Outlined in Table 1 are all the ore mineral phases, their chemical formula, and the mineral abbreviations used in the subsequent sample descriptions and figures. Outlined below are descriptions of all thin sections from the 1806 Zone.

Table 1. Sulfide minerals present within the 1806 Zone of the Ming VMS deposit as deduced from reflected light microscopy.

Predominant Phases	Mineral Abbreviation	Formula	Moderate to Trace Phases	Mineral Abbreviation	Formula
Arsenopyrite	Asp	FeAsS	Bismuthinite	Bis	Bi_2S_3
Chalcopyrite	Ccp	$CuFeS_2$	Boulangerite	Boul	$Pb_5Sb_4S_{11}$
Galena	Gn	PbS	Chalcocite	Cc	Cu_2S
Pyrite	Py	FeS_2	Covellite	Cov	CuS
Pyrrhotite	Po	$Fe_{1-x}S$	Gold	Au	Au
Sphalerite	Sp	ZnS	Hematite	Hem	Fe_2O_3
Tetrahedrite	Tet	$(Cu,Fe)_{12}Sb_4S_{13}$	Magnetite	Mag	Fe_3O_4
			Mawsonite	Maw	$Cu_6Fe_2SnS_8$
			Stannite	Stn	Cu_2FeSnS_4
			Tenantite	Ten	$(Cu,Fe)_{12}As_4S_{13}$

All phases are listed in alphabetical order not in order of abundance

Sample: 36501 (RMUG08-139, 36.7-36.77)

Hand Specimen Description: *Stringer pyrite-galena-sphalerite-arsenopyrite in lapillistone with quartz-sericite-carbonate gangue.*

Minerals: Py>Asp>Sp≈Gn>Ccp>Boul>Tet

Description:

Euehdral pyrite and arsenopyrite make up the bulk of this sample and are proximal to all other phases (Fig. 1). Most pyrite is recrystallized, larger, and has annealed textures with beautiful triple junctions between grains (Fig. 1). There is an intimate association of pyrite with arsenopyrite with arsenopyrite intergrown with pyrite with pyrite patches within larger arsenopyrite grains, and arsenopyrite intergrown as inclusions within larger pyrite grains (Fig. 1). Arsenopyrite also occurs as needles and diamonds that form separate crystals but are spatially proximal and intergrown with pyrite (Fig. 1). Sphalerite and galena are intergrown with pyrite and arsenopyrite and typically form anhedral masses between the grains of the latter (Fig. 1). Sphalerite also occurs as inclusions within pyrite and arsenopyrite (Fig. 1). Some galena and sphalerite grade into the masses of pyrite and have cuniform textures with rounded sphalerite-galena

inclusions within pyrite (Fig. 1). Boulangerite often occurs as inclusions within masses of arsenopyrite and chalcopyrite as soft, white-bluish green masses. Chalcopyrite is intergrown with galena-sphalerite-tetrahedrite and forms anhedral masses around pyrite and arsenopyrite grains (Fig. 1); it also occurs as blebs in sphalerite as chalcopyrite disease. Tetrahedrite is a minor phase but is found intergrown the galena-chalcopyrite-sphalerite and as anhedral exsolution blebs within galena (Fig. 1).

Sample: 36502 (RMUG08-139, 40.00-40.04m)

Hand Specimen Description: ***Chalcopyrite-pyrite-sulfosalt-rich ores with gangue.***

Minerals: Py≈Ccp>Sp>Tet>Boul>Asp>Gn

Description:

Pyrite and chalcopyrite are the dominant phases in this sample (Fig. 2). Pyrite is intergrown with other phases and is typically euhedral to subhedral forming large porphyroblasts down to smaller grains intergrown with chalcopyrite, sphalerite, tetrahedrite, and other phases (Fig. 2). Many larger pyrite masses are annealed with inclusions of the aforementioned sulfides (Fig. 2). Arsenopyrite is abundant occurring as euhedral intergrowths with pyrite, and as euheral porphrybolasts, the latter often containing inclusions of other phases (Fig. 2). Chalcopyrite occurs as myrmekitic intergrowths with tetrahedrite, boulangerite, galena, sphalerite, and arsenopyrite (Fig. 2). Often chalcopyrite forms the base to atolls and grainy intergrowths of chalcopyrite-tetrahedrite-sphalerite-arsenopyrite-pyrite in a sea of tetrahedrite (Fig. 2); in other samples these intergrowths are associated with Au. Tetrahedrite is very abundant in this sample and has myrmekitic intergrowths with chalcopyrite and a strong association with boulangerite and arsenopyrite (Fig. 2). Sphalerite, like other phases, occurs intergrown with the above phases (Fig. 2).

Sample: 36503 (RMUG08-139, 43.53-43.57 m)

Hand Specimen Description: ***Honey sphalerite stringers in between fragments of rhyolite.***

Minerals: Ccp≈Sp>Po>Py>>Gn>Bis≈Boul>>Cc

Description:

This section consists of intergrown chalcopyrite, sphalerite, pyrrhotite, pyrite with pyrrhotite forming bands within a sphalerite-rich zone in the section (Fig. 3). Sphalerite-pyrrhotite-chalcopyrite are all anhedreal and blebby and do not have well developed crystal faces (Fig. 3). Pyrite, in contrast, forms euhedral to subhedral crystals with inclusions of other phases, but is also present as inclusions within sheets of sphalerite (Fig. 3). Along some chalcopyrite grains there are needles of pyrrhotite intergrown and minor tarnished covellite and bismuthinite (Fig. 3). Tarnished bismuthinite (and covellite) is present in many chalcopyrite grains as blotches and along grain margins (Fig.

3); tarnished bismuthinite is always restricted to sections that contain pyrrhotite and those that have been contact metamorphosed by mafic dykes. There is minor anhedral galena associated with sphalerite grains and minor boulangerite pits in sphalerite-chalcopyrite-rich sulfides. Chalcocite is very rare in the 1806 Zone, but is present in very minor abundance along chalcopyrite-bismuthinite grain boundaries. Apatite is a common gangue phase and forms clasts and fragments within the ore.

Sample: 36504 (RMUG08-139, 44.28-44.32 m)

Hand Specimen Description: ***Buckshot sulfides with pyrrhotite, sphalerite, pyrite, arsenopyrite, and chalcopyrite.***

Minerals: Po>Py≈Sp>Ccp>Gn>Boul

Description:

This sample is dominated by pyrrhotite groundmass with porphryoblasts of euhedral pyrite that grows over all other phases and contains inclusions of chalcopyrite, sphalerite, pyrrhotite, galena, and boulangerite (Fig. 4). Pyrite porphyroblasts shows strong annealing with well-developed triple junctions between crystals with structural fabrics wrapping around grains but also being overgrown by the porphyroblasts (Fig. 4). Chalcopyrite and sphalerite are intergrown with one another in between pyrite and pyrrhotite grains with or without galena (Fig. 4). Boulangerite is very minor in this sample but does occur as blebs in chalcopyrite (Fig. 4).

Sample: 36505 (RMU08-138, 42.84-42.88 m)

Hand Specimen Description: ***Sphalerite-rich sulfides with galena, arsenopyrite, and sulfosalts.***

Minerals: Sp>Py>Ccp>Gn≈Tet≈Asp>Boul

Description:

Sphalerite is the dominant phase in this sample and is anhedral and proximal or hosts all other phases (Fig. 5). Pyrite is the next most abundant phase and occurs as euhedral grains and as porphyroblasts; the pyrie is variably annealed and often contains intergrowths and inclusions of sphalerite and arsenopyrite. (Fig. 5) In sphalerite there are small pyrite grains and there are often blebby intergrowths of small, euhedral arsenopyrite needles with tetrahedrite, chalcopyrite, sphalerite, and pyrite in a chalcopyrite host (Fig. 5). Arsenopyrite is found as grains within pyrite, near pyrite edges, and as porphyroblasts with relict fragments of pyrite in the porphyroblasts (Fig. 5). Chalcopyrite is found within the groundmass with sphalerite but is always intergrown with anhedral tetrahedrite and boulangerite (Fig. 5). Rarely, galena is present within the sphalerite-chalcopyrite-tetrahedrite intergrowth. Tetrahedrite has a greenish hue in this section, suggesting that it may be closer to tennantite than tetrahedrite, and exhibits an excellent polishing cleavage with anhedral boulangerite clots within it (Fig. 5). Boulangerite appears like galena in this section but has a bluish-green tint and is

anisotropic and is always associated with tetrahedrite and chalcopyrite (Fig. 5). Galena is abundant as white, anhedral clots in the sphalerite-pyrite-rich portion of the section; rarely is it proximal to chalcopyrite (Fig. 5).

Sample: 36506 (RMUG08-138, 46.71-46.74 m)

Hand Specimen Description: Buckshot sulfides with pyrite, pyrrhotite, and sphalerite

Minerals: Sp>Po>Py>Ccp>Gn

Description:

This section is dominated by sphalerite with intergrowths of blebby pyrrhotite and much lesser chalcopyrite (Fig. 6). Chalcopyrite is restricted to pyrite grain edges. Pyrite also occurs as euhedral to subhedral grains that range from small crystals to large porphyroblasts that have blebs of anhedral sphalerite within them (e.g., Swiss-cheese textures)(Fig. 6). Chalcopyrite occurs as blebs in pyrrhotite and in sphalerite and along pyrite grains (Fig. 6). It also occurs intergrown with galena, but this is relatively rare. Galena occurs as blebs in sphalerite.

Sample: 36507 (RMUG08-120, 54.2-54.24 m)

Hand Specimen Description: ***Sphalerite-pyrite-sulfosalt-rich sulfides***

Minerals: Sp≈Py>>Ccp>Boul>Asp>Tet

Description:

Sphalerite and pyrite are in subequal proportions in this sample. Sphalerite occurs as anhedral sheets and occurs between all phases and hosts pyrite and other phases (e.g., intergrown with other minerals)(Fig. 7). Pyrite crystals are of variable sizes but are euhedral to weakly subhedral and contain abundant ameboidal inclusions of sphalerite and boulangerite; pyrite grains often have cuniform-like textures with the included sphalerite (Fig. 7). Arsenopyrite grains are often near pyrite grains as euhedral intergrowths and along pyrite margins as euhedral, silvery white grains, often triangular, needle-like, and diamond-shaped (Fig. 7). Rare tetrahedrite grains occur near arsenopyrite-chalcopyrite-boulangerite intergrowths. Chalcopyrite is anhedral and occurs in betweeh pyrite grains and sphalerite, it is often intergrown with bluish-white boulangerite; boulangerite is always associated with chalcopyrite in this sample and is never a solitary phase (Fig. 7).

Sample: 36508 (RMUG08-120, 55.88-55.93 m)

Hand Specimen Description: ***Pyrite-rich sulfides with arsenopyrite, tetrahedrite, chalcopyrite; Au-rich zone.***

Minerals: Py>Sp≈Ccp>Asp>Tet>Boul

Description:

This section is dominated by massive, variably sized, euhedral and annealed pyrite cubes (Fig. 8). The pyrite crystals have well developed intergrowth textures with grains of pyrite surrounded by and intergrown with sphalerite, chalcopyrite, tetrahedrite, and boulangerite (Fig. 8). Arsenopyrite occurs as euhedral porphyroblasts that overgrow the matrix and contain inclusions of pyrite (Fig. 8). In between the pyrite and arsenpopyrite grains are anhedral masses of sphalerite, chalcopyrite, tetrahedrite, boulangerite, aresenopyrite and galena (Fig. 8). Chalcopyrite occurs in between pyrite and arsenopyrite and is commonly intergrown with galena, sphalerite, tetrahedrite and boulangerite; tetrahedrite and boulangerite are always associated with chalcopyrite (Fig. 8). This sample also contains atoll-like intergrowths, like other samples, with chalcopyrite, tetrahedrite, arsenopyrite, and sphalerite (Fig. 8). Galena is rare in this section but does occur as anhedral blebs in sphalerite and chalcopyrite (Fig. 8).

Sample: 36509 (RMUG08-120, 56.48-56.52 m)

Hand Specimen Description: ***Pyrite-arsenopyrite-tetrahedrite-rich sulfides with black material within it.***

Minerals: Py≈Tet>Asp>Sp≈Ccp >Gn>Boul>Au

Description:

This sample consists predominantly of euhedral pyrite that is intimately intergrown with euhedral grains of arsenopyrite occurring along pyrite edges and as inclusions within pyrite (Fig. 9). Arsenopyrite occurs in pyrite but also as large porphryoblasts that have pyrite inclusions and are much larger in size than pyrite (Fig. 9). Pyrite and arsenopyrite contain inclusions of other phases and it appears that both had multiple periods of mineral growth (Fig. 9). There is abundant tetrahedrite in this section occurring as anhedral sheets that cross the section and engulf other phases, except the arsenopyrite porphryroblasts (Fig. 9). Tetrahedrite is intergrown with galena, sphalerite, chalcopyrite, and boulangerite (Fig. 9); it forms up to 30-45% of the sulfide assemblage. Sphalerite is intergrown with tetrahedrite, galena, boulangerite, and chalcopyrite and has inclusions of pyrite (and vice versa) (Fig. 9). Galena has inclusions of pyrite (Fig. 9) also anhedral tetrahedrite exsolution blebs. Boulangerite is always intergrown with and present near chalcopyrite and tetrahedrite (Fig. 9). Chalcopyrite is anhedral and intergrown with other phases in between euhedral pyrite and arsenopyrite (Fig. 9). Gold is present in this section and is soft, is heavily scratched and pitted and is often tarnished (Fig. 9). It is found as anhedral belbs on the edges of arsenopyrite and pyrite porphyroblasts (Fig. 9).

Gold also occurs as blebs within arsenopyrite and along arsenopyrite edges where it is intergrown with boulangerite (Fig. 9).

Sample: 36510 (RMUG08-120, 59.61-59.65 m)

Hand Specimen Description: ***Pyrite-arsenopyrite-chalcopyrite-rich sulfides with pyrite much greater than arsenopyrite and chalcopyrite.***

Minerals: Py>Gn≈Asp≈>Tet>Sp>Ccp>Boul

Description:

This sample is dominated by euhedral recrystallized and annealed pyrite that is in most cases touching one another and forming larger pyritic masses with other sulfides phases occurring interstitial (Fig. 10). Arsenopyrite is less common than pyrite but occurs intergrown with pyrite or as larger porphryoblasts (Fig. 10). In between the pyrite grains is abundant, bright white galena that is much more abundant than all other sulfide phases (Fig. 10). Galena is anhedral and intergrown with anhedral tetrahedrite and lesser chalcopyrite and sphalerite (Fig. 10). Boulangerite is less common in this section that other sections but does occur proximal to tetrahedrite and chalcopyrite (Fig. 10). Galena, tetrahedrite, and sphalerite form myrmekitic intergrowths in parts of this section similar to the atoll-like structures in other sections (Fig. 10).

Sample: 36511 (RMUG08-120, 60.22-6025 m)

Hand Specimen Description: ***Galena-sphalerite-chlorite-rich sulfides that are variably foliated.***

Minerals: Py>Gn>Asp>Ccp>Sp> Tet>Boul>Au? or Bis?

Description:

Strongly foliated sample with layering of galena-rich zones with pyrite-rich layers that containing pyrite and arsenopyrite (Fig. 11). In part of the section galena has an anhedral, sheet-like nature with chloritic gangue and pyrite and arsenopyrite porphyroblasts with galena inclusions (Fig. 11). The galena also contains blebs of chalcopyrite and irregular patches of tetrahedrite as both exsolution blebs and as myrmekitic intergrowths of chalcopyrite, tetrahedrite, galena, and pyrite (Fig. 11). Pyrite forms large porphyroblasts but is also intergrown with arsenopyrite forming bands of pyrite and arsenopyrite (Fig. 11). Arsenopyrite crystals are also present as fine needles proximal to tetrahedrite and chalcopyrite (Fig. 11). Chalcopyrite and sphalerite are intergrown with tetrahedrite and galena and also occur as inclusions within rounded pyrite grains (e.g., cuniform inclusions in pyrite) (Fig. 11). Both phases also occur as irregular sheets in between pyrite grains. Tetrahedrite occurs in gangue with chalcopyrite and as belbs in galena (Fig. 11). Some potential flames of Au occur within tetrahedrite in gangue-rich bands (Fig. 11). Boulangerite is rare but is associated with chalcopyrite and tetrahedrite in a few locations in this sample.

Sample: 36512 (RMUG08-123, 59.48-59.33 m)

Hand Specimen Description: *Sphalerite-galena-rich sulfides.*

Minerals: Py>Sp>Gn≈Asp>Ccp>Stn

Description:

Euhedral pyrite and arsenopyrite are the predominant phases in this sample with abundant anhedral sphalerite that is intergrown with galena (Fig. 12). Pyrite contains inclusions of both galena and sphalerite and is intergrown with arsenopyrite along grain boundaries (Fig. 12). Aresnopyrite is euhedral, silvery white and occurs as needles and diamonds intergrown with pyrite and as porphyroblasts that in some cases include inclusions of pyrite. Arsenopyrite also occurs as grains within quartz-rich gangue, as latticeworks of needles, and also as fine needles near chalcopyrite and sphalerite (Fig. 12). Sphalerite and galena are very abundant and occur as anhedral masses that have myrmekitic intergrowth textures and both occur between pyrite grains and as sheets that host pyrite and arsenopyrite (Fig. 12). Chalcopyrite occurs predominantly within the quartz-rich gangue portion of this sample and as anhedral grains intergrown with galena, sphalerite, and pyrite (Fig. 12). In the chalcopyrite and sphalerite are anhedral, olive-brown to pinkish beige grains that are weakly pleochroic and have anoisotropy in bluish to reddish orange – these grains are likely stannite based on optical properties and from similar relationships in other sections. They occur along chalcopyrite edges and within chalcopyrite and form stannite disease in chalcopyrite when present (Fig. 12).

Sample: 36513 (RMUG08-123, 63.09-63.14 m)

Hand Specimen Description: *Pyrite-chalcopyrite-rich sulfides within Au-rich section.*

Minerals: Py>Ccp>Gn≈Asp≈Tet>Boul>Au

Description:

This sample contains abundant pyrite and arsenopyrite as euhedral crystals with interstitial chalcopyrite, tetrahedrite, boulangerite, galena and sphalerite (Fig. 13). Pyrite forms euhedral cubes that are variably annealed and touching with edges between grains filled with other sulfide phases (Fig. 13). The pyrite often have latticeworks with partial replacement and fence-like distributions of chalcopyrite (Fig. 13). Arensopyrite is abundant occurring as fine needles and euhedra proximal to pyrite but also in chalcopyrite and sphalerite; more rarely they form large, euhedral porphryoblasts (Fig. 13). Sphalerite is not as abundant as in other sections and occurs in one part of the section as a large sheet intergrown with pyrite, galena, chalcopyrite, and arseopyrite. Sphalerite is also intergrown with chalcopyrite, pyrite, and other sulfide phases as smaller anhedral grains as well. Anhedral galena is abundant and intergrown with chalcopyrite, tetrahedrite, pyrite, arsenopyrite, tetrahedrite and boulangerite (Fig. 13). Tetrahedrite is very abundant and intergrown with chalcopyrite along grain boundaries and as exsolution blebs in galena (Fig. 13). Chalcopyrite forms much of the interstitial material between

chalcopyrite-pyrite grains and boulangerite is typically found within chalcopyrite, and in chalcopyrite-tetrahedrite intergrowths (Fig. 13). Gold is found in numerous locations within this sample, typically as rounded, pitted grains always with chalcopyrite-tetrahedrite-arsenopyrite assemblages (Fig. 13). This Au-sulfide assemblage typically occurs along chalcopyrite grain edges proximal to pyrite and arsenopyrite and consists of raspberry-like structures with chalcopyrite, blebby tetrahedrite, and fine arsenopyrite needles with rounded grains of Au (Fig. 13).

Sample: 36514 (RMUG08-123, 63.54-63.59 m)

Hand Specimen Description: *Pyrite-sulfosalt-galena-rich sulfides.*

Minerals: Py>Gn>Tet>Ccp≈Asp>Sp>Boul

Description:

This sample is banded with abundant pyrite, galena and other phases (Fig. 14). Pyrite is euhedral and forms the bulk of the section and has annealed textures and some rounded grains with inclusions of galena, sphalerite, and chalcopyrite (Fig. 14). Arseonpyrite is intergrown with pyrite as elongate grains and/or euhedral diamond shaped crystals, often near sulfosalts, and as very fine needles within gangue (Fig. 14). Galena forms a large part of the sample as anhedral grains, typically interstitial to pyrite and containing inclusions of pyrite; galena often exhibits intergrowths with sphalerite, chalcopyrite, tetrahedrite, and boulangerite, as well (Fig. 14). Sphalerite and chalcopyrite are small grains, anhedral grains intergrown with galena (Fig. 14). Tetrahedrite is abundant, is greenish-grey in colour, is intergrown with galena, and occurs as exsolved flames and blebs within galena, where it is less greenish and more grey in colour (Fig. 14). Boulangerite is relatively minor, but is typically proximal to and/or hosted by tetrahedrite and chalcopyrite (Fig. 14).

Sample: 36515 (RMUG08-123, 63.63-63.67 m)

Hand Specimen Description: *Chalcopyrite-pyrite-arsenopyrite-rich sulfides.*

Minerals: Ccp>Py>Gn≈Sp≈Asp>Tet>Bis>Ten

Description:

This sample is dominated by chalcopyrite sheets that are cutting, hosting, or are intergrown with other phases (Fig. 15). Chalcopyrite has myrmekitic intergrowths with sphalerite and galena and is associated with euhedral pyrite along chalcopyrite grain edges and within chalcopyrite grains. In more gangue-rich zones euhedral pyrite is associated with sphalerite, chalcopyrite, galena along grain edges (Fig. 15). Euhedral porphryblasts of arsenopyrite occur within chalcopyrite sheets (Fig. 15) and arsenopyrite also occur as small needles, triangles, and diamonds that are intergrown with pyrite or spatially proximal to pyrite; fine needles are also present in the gangue as well. Anhedral sphalerite and galena are intergrown with one another and within chalcopyrite (Fig. 15). This section also contains bismuthinite that is soft, bright white to yellowish, and highly

anisotropic that is intergrown with chalcopyrite and contains inclusions of chalcopyrite, and proximal to sphalerite (Fig. 15). Bismuthinite also contains a well-developed rind of greenish-grey tennantite that is highly anisotropic, with deep red internal reflections (Fig. 15). Tetrahedrite is present as inclusions within sphalerite and exsolution blebs in galena.

Sample: 36516 (RMUG08-125, 49.56-49.61 m)

Hand Specimen Description: *Galena-sphalerite-chacopyrite-rich sulfides with sulfosalts.*

Minerals: Sp≈Gn≈Py>>Asp>Ccp

Description:

This sample consists of abundant euhedral pyrite intergrown with sphalerite-galena-arsenopyrite (Fig. 16). Pyrite is variably annealed and contains inclusions of other sulfide phases (Fig. 16). Arsenopyrite occurs as inclusions in pyrite, as euhedral crystals near pyrite, and as porphyroblasts in galena-sphalerite sheets (Fig. 16). Anhedral sphalerite and galena are intergrown with one another and exhibit myrmekitic textures (Fig. 16). Some chalcopyrite as anhedral inclusions along sphalerite-galena grain edges and intergrown with galena and sphalerite (Fig. 16). Tetrahedrite occurs as exsolution blebs within galena grains (Fig. 16).

Sample: 36517 (RMUG08-125, 52.09-52.13 m)

Hand Specimen Description: *Pyrite-sphalerite-chalcopyrite-arsenopyrite-rich sulfide.*

Minerals: Py>Sp>Ccp≈Gn≈Boul>Asp>Tet

Description:

This sample has abundant pyrite and arsennopyrite grains withina matrix of intergrown sphalerite, chalcopyrite, and galena (Fig. 17). Pyrite is euhedral to weakly subhedral and has inclusions of galena, sphalerite, chalcopyrite and is annealed and recrystallized (Fig 17). Some pyrite forms polycrystalline aggregates around sphalerite with sphalerite forming an island within a rim of pyrite grains (Fig. 17). Arsenopyrite occurs as euhedral crystals with pyrite and as well as fine latticeworks of needles (Fig. 17). Sphalerite is anhedral and occurs as sheets intergrown with galena and chalcopyrite where they exhibit myrmekitic textures (Fig 17). Galena and sphalerite exhibit similar textures (Fig. 17). Boulangerite present primarily as irregular belbs within chalcopyrite and looks similar to galena except for it has pleochroism, anisotropy, and a bluish-green hue (Fig. 17). Tetrahedrite is relatively minor in this sample and occurs primarily as exsolution blebs with galena grains (Fig. 17).

Sample: 36518 (RMUG08-125, 54.26-52.29 m)

Hand Specimen Description: *Pyrite-sphalerite-arsenopyrite-chalcopyrite-bearing sulfide*

Minerals: Py>Sp≈Tet>Gn≈Ccp>Boul>Asp>Au>Bis?

Description:

This is a very complex section but a key one for understanding the sulfide mineralogy of the 1806 Zone and contains a wide variety of sulfides, sulfosalts, and native elements. Pyrite is very abundant and is euhedral to subhedral, varreably annealed, and has cuniform, wormy inclusions of sphalerite, chalcopyrite, galena, and other phases (Fig. 18). Pyrite is spatially associated with arsenopyrite in many parts of the section where the latter occurs as euehdral grains with pyrite inclusions or as solitary grains in with pyrite (Fig. 18). Arsenopyrite also occurs as latticeworks of needles surrounding chalcopyrite crystals and as euhedral grains intergrown in atoll-like structures with chalcopyrite, arsenopyrite, sphalerite, and tetrahedrite (Fig. 18). Arsenopyrite also forms euhedral grains in chalcopyrite with nearby boulangerite, tetrahedrite, and Au (Fig. 18). Sphalerite, galena, and chalcopyrite are intergrown with one another within the matrix of the rock occur as anhedral sheets with anhedral grains of these phases (Fig. 18). Sphalerite and tetrahedrite are typically associated with aggregates of chalcopyrite with arsenopyrite, tetrahedrite, boulangerite and Au (Fig. 18). Gold also occurs inside of some arsenopyrite grains and boulangerite is present as inclusions in some chalcopyrite grains associated with tetrahedrite (Fig. 18). Tetrahedrite is very abundant in this section and is associated with sphalerite, galena, and chalcopyrite forming larger sheets as well as exsolution blebs in galena; the latter is the less common form (Fig. 18). Stannite is present in a few localities within this sample as small inclusions boulangerite or galena, and as similar inclusions in tetrahedrite (Fig. 18). Bismuthinite(?) occurs on the edge of a chalcopyrite grain within sphalerite as a small iridescent irregularly shaped grain (Fig. 18); this mineral is very minor in this section. Arsenopyrite and boulangerite contain very small, and very rare, orange-brown pleochroic blebs that have anisotropism in yellow that may be mawsonite.

Sample: 36519 (RMUG08-125, 55.28-55.23 m)

Hand Specimen Description: *Pyrite-arsenopyrite-tetrahedrite-rich sulfides*

Minerals: Py>Ccp>Tet≈Gn≈Sp>Asp>Boul≈Au≈Stn>>Maw

Description:

This section contains abundant euhedral pyrite that is well annealed and has amazing triple junctions between grains (Fig. 19). Arsenopyrite is euhedral and and intergrown with pyrite occurring either as needles, diamond-shaped grains, or as large grains with inclusions of pyrite, boulangerite and chalcopyrite (Fig. 19). Galena is intergrwon with tetrahedrite and there is abundant chalcopyrite, sphalerite (with chalcopyrite disease), and galena in between pyrite grains (Fig. 19). Tetrahedrite is associated with masses of

chalcopyrite, boulangerite, maswonite and grains of stannite (Fig. 19). Boulangerite is restricted to chalcopyrite and tetrahedrite and has greenish hues and anisotropism. Stannite is present in numerous locations in this sample but is commonly associated with boundaries near tetrahedrite and galena or near chalcopyrite and sphalerite boundaries, there are also stannite blebs in sphalerite as well (Fig. 19). Gold is present spatially associated with chalcopyrite-tetrahedrite-arsenopyrite assemblages forming rounded grains within chaclpyrite near arsenopyrite and tetrahedrite or within the other phases (Fig. 19). Mawsonite is rare but present as very small, irregular blebs along he margins of boulangerite.

Sample: 36520 (RMUG08-142, 60.51-60.55 m)

Hand Specimen Description: *Grainy, pyritic sulfides.*

Minerals: Py>Sp>Ccp>Asp>Boul>Gn>Tet>Au>>Stn/Maw

Description:

This section is dominated by fine to medium grained, euhedral and densely packed, annealed pyrite with amazing triple junctions (Fig. 20). In between the triple junctions are various phases as anhedral grains, including sphalerite, galena, chalcopyrite, arsenopyrite, boulangerite, Au, and bismuthinite (Fig. 20). Arsenopyrite crystals are restricted to inter-pyrite locales and form euhedral needles and triangular grains in with gangue (Fig. 20). Sphalerite forms interstitial, anhedral blebs and always has chalcopyrite disease and is often itnergrown with galena, chalcopyrite, and/or gold (Fig. 20). Chalcopyrite is similar to sphalerite but locally contains greenish blebs of boulangerite (Fig. 20). Gold is remarkably abundant in this sample and occurs in triple junctions forming to the shape of the pyrite grains and is often intergrown with bismuthinite that exhibits iridescence (Fig. 20); rarely is gold found within the pyrite grains. Boulangerite is found in chalcopyrite but more rarely is found on its own in between pyrite grains (Fig. 20). Tetrahedrite is rare but presented on the edge of sphalerite grains near gauge as a linear intergrowth with chalcopyrite and stannite (or mawsonite occurs in one location proximal to a contact between sphalerite, galena, and pyrite (Fig. 20).

Sample: 36522 (RMUG08-142, 63.53-65.57 m)

Hand Specimen Description: *Buckshot sulfides with pyrite, pyrrhotite, and sphalerite*

Minerals: Py≈Po>Ccp>Sp>Gn≈Mag≈Bis≈Boul

Description:

Thei sample consists predominantly of pyrite, pyrrhotite, and chalcopyrite with chalcopyrite forming anhedral sheets intergrown with pyrrhotite and pyrite (Fig. 22). Pyrite occurs as large buckshot porphyroblasts that contain inclusions of pyrite, chalcopyrite, sphalerite, galena, bismuthinite, and very rarely pyrrhotite (Fig. 22). Pyrite

porphyryoblasts also contain cracks that are often filled with pyrrhotite with or without chalcopyrite and boulangerite, the latter always intergrown with chalcopyrite (Fig. 22). Pyrite also forms euhedral grains intergwon with chalcopyrite and pyrrhotite (Fig. 22). Pyrrhotite occurs as large sheets with inclusiosn of other phases including the pyrite porphyroblasts, chalcopyrite, and sphalerite (Fig. 22). Sphalerite is present as irregular blebs intergrown with pyrrhotite and as inclusions in pyrite porphyroblasts (Fig. 22). There is abundant tarnishing to iridescence associated with a whitish yellow mineral in chalcopyrite that likely is bismuthinite (Fig. 22). Magnetite is present as euhedral to anhedral grains in pyrrhotite and often contains inclusions of pyrrhotite (Fig. 22). Hematite occrs along fractures in some parts of this sample, although this is a minor phase.

Ore Mineral Summary: Primary versus Secondary Ore Minerals

Deformation has played a role in upgrading and changing the mineralogy and texture of much of the sulfides within the 1806 Zone; however, most of the minerals were likely primary to the VMS forming system but were subsequently upgraded and recrystallized due to deformation and metamorphism. It is likely that all sulfide, sulfosalt, and native metals were primary (see arguments below), with the exception of pyrrhotite, magnetite, hematite, and bismuthinite, which are restricted to the buckshot ore samples or near buckshot ore samples, or those that have been deformed. For example, bismuthinite is always associated with chalcopyrite, but is only present in samples that have a deformation fabric or have a pyrrhotite-buckshot pyrite assemblage. Similarly, magnetite and hematite are restricted to pyrrhotite-rich sulfides and pyrrhotite-rich samples are only present in areas where the sulfide minerals come in contact with mafic dykes.

The common occurrence of tetrahedrite/tennantite-boulangerite-stannite-mawsonite-arsenopyrite-Au associated with normal VMS assemblages of sphalerite-pyrite-chalcopyrite-galena suggests that these minerals were precipitated as primary phases during the formation of the VMS deposit, rather than formed due to metamorphic recrystallization. Metamorphic recrystallization was likely important in mobilizing Au (see below), and was likely important in the growth and recrystallization of both pyrite and arsenopyrite, and the formation of myrmekitic textures between other sulfides phases.

Key Gold Mineral and Textural Associations in the 1806 Zone and the Origins of Gold Enrichment in the 1806 Zone

Gold is very enriched in the 1806 Zone when compared to most VMS deposit, illustrating why Rambler is considered a Au-rich VMS deposit by many workers (Dubé et al., 2007a; Hannington et al., 1999b; Poulsen and Hannington, 1995). Gold in the 1806 Zone occurs in association with different phases, but has a few key associations: 1) gold is associated with atoll-like intergrowths of chalcopyrite, tetrahedrite, and arsenopyrite with or without sphalerite (e.g., Fig. 13); 2) gold occurs as grains within and along the edges of tetrahedrite grains (e.g., Fig. 11f); 3) gold is spatially associated with arsenopyrite porphyryblasts and tetrahedrite, chalcopyrite, and boulangerite (Figs. 18h-k); and

4) gold is present in between grains of pyrite and arsenopyrite either by itself or intergrown with boulangerite or bismuthinite (e.g., Figs. 9f and 20e-f). In all cases Au is spatially associated with arsenopyrite and sulfosalt phases. In the fourth case, however, Au is associated with structural void space in between annealed arsenopyrite and pyrite crystals. In all cases gold is spatially associated with grain margins and not in the cores of mineral grains, suggesting the potential for liberation; further testing of milled concentrates is required to prove this hypothesis.

The origins of Au within the Rambler VMS camp has been controversial with some workers favouring a primary, syn-VMS origin (Santaguida and Hannington, 1996), whereas others suggest the potential for an orogenic overprint (Weick, 1993). The confusion and suggestion of an orogenic overprint likely arises from the fact that there are numerous orogenic vein-style Au deposits in the Baie Verte area (e.g., Pine Cove, Deer Cove)(e.g., Evans et al., 1998; Patey and Wilton, 1993; Ramezani et al., 2000), and the fact that the Rambler deposits are strongly deformed (Tuach, 1988). While it is possible that orogenic overprints have occurred in this area, the lack of carbonate alteration and the association of Au with sulfide minerals, rather than quartz-carbonate veins (e.g., Poulsen et al., 2000), argues strongly against an orogenic origin for the Au. Deformation was likely important, however, in mobilizing Au, recrystallizing pyrite and arsenopyrite, and liberating Au (e.g., Fig. 9, 20)(Larocque et al., 1993; Santaguida and Hannington, 1996; Wagner et al., 2007), especially for the Au associated with annealed pyrite and arsenopyrite and their grain margins.

The origin of Au in this 1806 Zone and the Rambler VMS camp likely was a function of a magmatic contribution to the VMS hydrothermal system that formed the Ming and other deposits in the belt. A number of lines of evidence support this hypothesis. The strong association of Au with tetrahedrite, arsenopyrite, chalcopyrite, bismuthinite, and boulangerite in the ores suggest Au associated with minerals enriched in Cu-As-Sb-Bi, elements that are largely associated with magmatic hydrothermal systems, rather than normal seafloor VMS hydrothermal systems (e.g., Hannington et al., 1999b). Furthermore, most of these elements, in addition to other magmatophile elements (e.g., Hg), show moderate to strong strong correlations with Au-Ag-enrichment in the 1806 Zone (Fig. 23). These mineral assemblages and elemental associations are strongly supportive of a magmatic fluid/volatile contribution as the as the cause of Au enrichment in the 1806 Zone. Furthermore, the presence of Sn-sulfosalts mawsonite and stannite are also supportive of a magmatic contribution to the Ming VMS system as Sn is one of the "smoking guns" indicating potential magmatic contributions to VMS systems (Boyle, 1997; Hannington et al., 1999a; Relvas et al., 2006a; Relvas et al., 2006b). Further work is required, but the current data support the hypothesis of a magmatic contribution as a cause of Au-Ag-enrichment in the Ming VMS deposit and 1806 Zone.

Comparisons to Other Gold-Rich VMS Systems

The 1806 Zone of the Ming VMS deposit is similar to many normal VMS deposits in containing a typical VMS-bearing assemblage of pyrite, chalcopyrite, sphalerite, and galena; however, this zone has unusual Au-Ag-enrichment, abundant arsenopyrite, and sulfosalt enrichment. The presence of abundant arsenopyrite and sulfosalts in association

with Au mineralization, and enrichments in magmatic suite elements (e.g., Cu-As-Sb-Hg) in the ores, are features that are common to many Au-rich VMS systems globally (e.g., Bousquet-LaRonde; Eskay Creek; Mount Lyell; Boliden)(Dubé et al., 2007a; Dubé et al., 2007b; Grammatikopoulos et al., 2005; Hannington et al., 1999b; Large et al., 1996; Large et al., 2001; Roth et al., 1999; Sillitoe et al., 1996; Wagner et al., 2007). The strongest comparison seems to be with the deposits of the Bousquet-LaRonde district in Quebec, at least in terms of the sulfide mineralogy (Table 2), geological and structural setting, and grade; notably, the deposits of the Bousquet-LaRonde district are significantly larger than those of the Rambler district. Shown for comparison is the sulfide mineralogy of the deposits of the Bousquet-LaRonde camp in comparison to that present in the 1806 Zone. A key feature to note here is that many of the minerals identified by Dubé et al. (2007a) were identified by micro-analytical methods (e.g., SEM, electron probe), many of these are likely in the 1806 Zone but not identifiable by normal optical microscopy. From this table it is clear the sulfides of the 1806 Zone have strong similarities to the deposits of the Bousquet-LaRonde camp, in particular the LaRonde deposit.

Table 2. Ore minerals present in the deposits of the Bousquet-LaRonde district in comparison to the 1806 Zone of the Ming VMS deposit. Table modified from Dubé et al. (2007a).

	LaRonde	**Bousquet 2**	**Dumagami**	**Bousquet 1**	***1806 Zone***
Major Minerals	Pyrite Pyrrhotite Chalcopyrite Sphalerite Galena	Pyrite Chalcopyrite Bornite	Pyrite Chalcopyrite Sphalerite	Pyrite Chalcopyrite	Pyrite Chalcopyrite Sphalerite Tetrahedrite
Minor Minerals	Arsenopyrite Tetrahedrite Stannite Magnetite	Sphalerite Galena Tennantite Chalcocite Pyrrhotite Magnetite	Galena Arsenopyrite Bornite Chalcocite Covellite Digenite	Sphalerite Pyrrhotite Magnetite Arsenopyrite Galena Bornite	Arsenopyrite Galena Pyrrhotite Boulangerite
Trace Minerals	Electrum Hessite Native Bi Bi-telluride Ag-Bi sulfide Cu-Pb-Bi sulfide Pb-Sb sulfosalts Ag-Sb sulfosalts Gudmundite Clausthalite Colusite Scheelite Cassiterite Clausthalite	Electrum Hessite Petzite Altaite Tellurobismuthinite Mawsonite Colusite Renierite	Electrum Altaite Cu-Ag sulfide Stannite Alabandite	Electrum Au-telluride Altaite Stannite Gudmundite	Gold (electrum) Bismuthinite Chalcocite Covellite Gold (Electrum) Hematite Magnetite Mawsonite Stannite Tennantite

Recommendations

Considerable knowledge has been gleaned about the nature of the ore mineralogy, Au-associations, and residence of different elements in the 1806 Zone of the Ming VMS deposit. Further examination of the ore mineralogy could be undertaken using microbeam methods, including the scanning electron microscope (SEM) and electron microprobe microanalysis (EPMA), this would provide further confirmation of existing observations, provide a better handle on any microscopic Au not visible via optical microscopy, and help identify other phases that may be of significance as potential hosts for precious metals or other deleterious elements. In addition, mineral liberation analysis (MLA) and imaging using the SEM could also be done at Memorial University and this would provide images of element and mineral residence but also a quantitative determination of the nature and abundance of sulfide-sulfosalt-precious mineral contents. While this work is expensive, it would provide significant insight into whether elements would be easily liberated or not during mining and milling. This may be more applicable, and in the authors opinion imperative, for the concentrate samples that are the subject of a complementary study to this one.

There is still considerable room for further field-based work to better understand the alteration system and geometry of the 1806 Zone and its relationship to other zones in the Ming deposit. Futhermore, there is also room for detailed studies of the assay database, and the potential for lithogeochemical and alteration studies on different zones within the Ming deposit. These are, of course, subject to funding and the scope of ongoing exploration and development.

Summary

The 1806 Zone of the Ming VMS deposit is a base- and precious-metal-enriched sulfide zone with Au-Ag-enrichment similar to many world-class Au-rich VMS systems. The ore mineralogy of the deposit is dominated by various sulfide, sulfosalt, native metal, and oxide phases. Sulfides are variably recrystallized due to deformation and metamorphism and are strongly recrystallized and contact metamorphosed in proximity to younger mafic dykes. Massive sulfide distal from dyke margins, despite being deformed and recrystallized, are likely representative of the primary VMS-bearing assemblage given typical VMS-related mineral assemblages that dominates the sulfides (e.g., pyrite-chalcopyrite-sphalerite-galena). These massive sulfides are dominated by variable amounts of sulfide (pyrite, chalcopyrite, sphalerite, galena, and arsenopyrite), sulfosalts (tetrahedrite, boulangerite, stannite, mawsonite, tennantite), and Au (electrum?). Massive sulfide that has been recrystallized and contact metamorphism in proximity to mafic dykes are characterized by buckshot textures with abundant pyrrhotite-rich sulfides with pyrite porphyroblasts, and lesser sphalerite, chalcopyrite, galena, sulfosalts, and magnetite. Notably, these buckshot ore samples are rich in iridescent bismuthinite and have a very minor amount of arsenopyrite, much lower than in the primary VMS-bearing sulfides.

Gold show four main associations in the 1806 Zone: 1) in association with atoll-like intergrowths of chalcopyrite, tetrahedrite, and arsenopyrite with or without sphalerite; 2)

within and along the edges of tetrahedrite grains; 3)spatially associated with arsenopyrite porphyryblasts and tetrahedrite, chalcopyrite, and boulangerite; and 4) between grains of pyrite and arsenopyrite either by itself or intergrown with boulangerite or bismuthinite. In all cases Au is spatially associated with arsenopyrite and sulfosalt phases. In the fourth case, however, Au is associated with structural void space in between annealed arsenopyrite and pyrite crystals. In all cases gold is spatially associated with grain margins and not in the cores of mineral grains, suggesting the potential for liberation; further testing of milled concentrates is required to prove this hypothesis. While deformation has played a role in remobilizing and potentially liberating Au (e.g., type 4 gold above), the strong association with arsenopyrite, Sb-As-rich sulfosalts, and magmatic element enrichments in assays (e.g., anomalous Cu-Sb-As-Hg-Ag) suggest that the Au was introduced by magmatic fluids and was not the product of an orogenic overprint as has been suggested by some other workers. The geological, mineralogical, and chemical attributes of the massive sulfides from the 1806 Zone are similar to other Au-Ag-rich VMS systems globally (e.g., Bousquet-LaRonde; Eskay Creek; Boliden; Mount Lyell), but the geological setting, ore mineralogy, and deformation style is most similar to the deposits of the Bousquet-LaRonde district in Quebec.

It is recommended that further microanalytical work (e.g., SEM, electron microprobe, mineral liberation analysis) be performed on these samples to further constrain the mineralogy, residence of precious metals and base metals, and the location and residence of potential deleterious elements. A concentrate study that complements this study is imperative to better understand the liberation of various phases in this deposit. Longer term, there is much potential to continue research into comparisons of the setting and massive sulfide mineralogy of different zones in the Ming deposit, their alteration envelopes, and to better understand the base, precious, and trace metal zoning within the 1806 and other zones in the Ming VMS system using the existing assay database.

References

Boyle, D. R., 1997, Distribution of tin in massive sulphide deposits of the Bathurst mining camp; exploration significance: Program with Abstracts - Geological Association of Canada; Mineralogical Association of Canada; Canadian Geophysical Union, Joint Annual Meeting, v. 22, p. 16-17.

Dubé, B., Gosselin, P., Mercier-Langevin, P., Hannington, M., and Galley, A., 2007a, Gold-rich volcanogenic massive sulphide deposits, *in* Goodfellow, W. D., ed., Mineral Deposits of Canada: A Synthesis of Major Deposit-types, District Metallogeny, the Evolution of Geological Provinces, and Exploration Methods, Special Publication 5, Mineral Deposits Division, Geological Association of Canada, p. 75-94.

Dubé, B., Mercier-Langevin, P., Hannington, M., Lafrance, B., Gosselin, G., and Gosselin, P., 2007b, The LaRonde Penna World-Class Au-Rich Volcanogenic Massive Sulfide Deposit, Abitibi, Quebec: Mineralogy and Geochemistry of

Alteration and Implications for Genesis and Exploration: Economic Geology, v. 102, p. 633-666.

Evans, D. T. W., Pereira, C. P. G., and Walsh, D. G., 1998, Epigenetic gold mineralization, Baie Verte Peninsula, Newfoundland: Current Research Report, Report: 98-1, pp.39-51, Mar 1998.

Grammatikopoulos, T. A., Roth, T., and Valeyev, O., 2005, Compositional variation in Hg–Ag-rich tetrahedrite from the polymetallic Eskay Creek deposit, British Columbia, Canada: Neues Jahrbuch fuer Mineralogie. Abhandlungen, v. 181, p. 281-292.

Hannington, M. D., Bleeker, W., and Kjarsgaard, I., 1999a, Sulfide mineralogy, geochemistry, and ore genesis of the Kidd Creek Deposit; Part I, North, Central and South orebodies: Economic Geology Monographs, v. 10, p. 163-224.

Hannington, M. D., Poulsen, K. H., Thompson, J. F. H., and Sillitoe, R. H., 1999b, Volcanogenic gold in the massive sulfide environment, *in* Barrie, C. T., and Hannington, M. D., eds., Volcanic-Associated Massive Sulfide Deposits: Processes and Examples in Modern and Ancient Settings, Reviews in Economic Geology 8: Littleton, CO, USA, Society of Economic Geologists, p. 325-356.

Large, R. R., Doyle, M., Raymond, O., Cooke, D., Jones, A., and Heaman, L., 1996, Evaluation of the role of Cambrian granites in the genesis of world class VHMS deposits in Tasmania: Ore Geology Reviews, v. 10, p. 215-230.

Large, R. R., McPhie, J., Gemmell, J. B., Herrmann, W., and Davidson, G. J., 2001, The spectrum of ore deposit types, volcanic environments, alteration halos, and related exploration vectors in submarine volcanic successions: some examples from Australia: Economic Geology, v. 96, p. 913-938.

Larocque, A. C. L., Hodgson, C. J., and Lafleur, P.-J., 1993, Gold distribution in the Mobrun volcanic-associated massive sulfide deposit, Noranda, Quebec; a preliminary evaluation of the role of metamorphic remobilization: Economic Geology, v. 88, p. 1443-1459.

Patey, K. S., and Wilton, D. H. C., 1993, The Deer Cove Deposit, Baie Verte Peninsula, Newfoundland, a Paleozoic mesothermal lode-gold occurrence in the Northern Appalachians: Canadian Journal of Earth Sciences = Journal Canadien des Sciences de la Terre, v. 30, p. 1532-1546.

Poulsen, H., and Hannington, M., 1995, Auriferous Volcanogenic Sulfide Deposits, *in* Eckstrand, O. R., Sinclair, W. D., and Thorpe, R. I., eds., Geology of Canadian Mineral Deposit Types, Geology of Canada, no. 8, P-1. Decade of North American Geology (DNAG), Geological Society of America, p. 183-196.

Poulsen, K. H., Robert, F., and Dube, B., 2000, Geological Classification of Canadian Gold Deposits, Bulletin 540: Ottawa, ON, Canada, Geological Survey of Canada, p. 113.

Ramezani, J., Dunning, G. R., and Wilson, M. R., 2000, Geologic setting, geochemistry of alteration, and U-Pb age of hydrothermal zircon from the Silurian Stog'er Tight gold prospect, Newfoundland Appalachians, Canada: Exploration and Mining Geology, v. 9, p. 171-188.

Relvas, J. M. R. S., Barriga, F. J. A. S., Ferreira, A., Noiva, P. C., Pacheco, N., and Barriga, G., 2006a, Hydrothermal Alteration and Mineralization in the Neves-Corvo Volcanic-Hosted Massive Sulfide Deposit, Portugal. I. Geology, Mineralogy, and Geochemistry: Economic Geology, v. 101, p. 753-790.

Relvas, J. M. R. S., Barriga, F. J. A. S., and Longstaffe, F. J., 2006b, Hydrothermal Alteration and Mineralization in the Neves-Corvo Volcanic-Hosted Massive Sulfide Deposit, Portugal. II. Oxygen, Hydrogen, and Carbon Isotopes: Economic Geology, v. 101, p. 791-804.

Roth, T., THompson, J. F. H., and Barrett, T. J., 1999, The precious metal-rich Eskay Creek deposit, northwestern British Columbia, *in* Barrie, C. T., and Hannington, M. D., eds., Volcanic-Associated Massive Sulfide Deposits: Processes and Examples in Modern and Ancient Settings, Reviews in Economic Geology, Volume 8, Society of Economic Geologists, p. 357-373.

Santaguida, F., and Hannington, M. D., 1996, Characteristics of gold mineralization in volcanogenic massive sulphide deposits of the Notre Dame Bay area, central Newfoundland: Canadian Journal of Earth Sciences, v. 33, p. 316-334.

Sillitoe, R. H., Hannington, M. D., and Thompson, J. F. H., 1996, High sulfidation deposits in the volcanogenic massive sulfide environment: Economic Geology, v. 91, p. 204-212.

Tuach, J., 1988, Geology and sulphide mineralization in the Pacquet Harbour Group, *in* Swinden, H. S., and Kean, B. F., eds., The volcanogenic sulphide districts of central Newfoundland, Geological Association of Canada, p. XX-XX.

Wagner, T., Klemd, R., Wenzel, T., and Mattsson, B., 2007, Gold upgrading in metamorphosed massive sulfide ore deposits: Direct evidence from laser-ablation-inductively coupled plasma-mass spectrometry analysis of invisible gold: Geology, v. 35, p. 775-778.

Weick, R. J., 1993, Petrography and stable isotope geochemistry of alteration and mineralization in the Rambler volcanogenic massive sulphide deposit, Baie Verte, Newfoundland: Unpub. Unpublished MSc Thesis thesis, Memorial University of Newfoundland and Labrador.

Important Notice

The quality of information, conclusions, and estimates contained herein is consistent with the level of effort involved in Stephen J. Piercey Geological Consulting's services, based on: i) information available at the time of preparation, ii) data supplied by outside sources, and iii) the assumptions, conditions, and qualifications set forth in this report. The results and opinions expressed in this report are based on Stephen J. Piercey Geological Consulting's interpretation of technical data sited in this report. While Stephen J. Piercey Geological Consulting has carefully reviewed all of the information provided by Rambler Metals and Mining Ltd., and believes the information to be reliable, Stephen J. Piercey Geological Consulting has not conducted an in-depth independent investigation to verify its accuracy and completeness.

This report is intended for Rambler Metals and Mining Ltd. and any third party use is at that party's sole risk.

Appendix A: Table of Minerals Present in Sulfide Samples and Assay Grades for Intervals Hosting Sulfide Samples

Sample	Drill Hole	From	To	Description	Asp	Bis	Boul	Ccp	Cc	Cov	Gn	Hem	Au	Mag	Maw	Py	Po	Sp	Stn	Ten	Tet	Notes	Au (g/t)	Ag (g/t)	Cu (%)	Pb (%)	Zn (%)
36501	RMUG08-139	36.7	36.77	Stringer py-ga-sph-aspy in felsic lapillistone	X		X	X			X					X		X			X	-	7.733	57.5	0.036		0.73
36502	RMUG08-139	40	40.04	Cpy-py-sulfosalt ores with gangue, aspy.	X		X	X			X					X		X			X	Atoll intergrowths	65.863	368.2	6.3		7.2
36503	RMUG08-139	43.53	43.57	Cpy-sph-ga sulfides		X	X	X	X	?	X					X	X	X				Metamorphosed? Buckshot	1.192	26.1	1.06		7.8
36504	RMUG08-139	44.28	44.32	Buckshot sulfides with Po-sph-py-aspy-cpy			X	X			X					X	X	X				-	2.876	95.1	0.52		35.6
36505	RMUG08-138	42.84	42.88	Sph-rich sulfide with ga-aspy-sulfosalts	X		X	X			X					X		X			X	Atoll intergrowths	27.055	395.1	1.76		23.1
36506	RMUG08-138	46.71	46.74	Buckshot sulfides with py-po-sph				X			X					X	X	X					31.09	46.4	0.6		13.6
36507	RMUG08-120	54.2	54.24	Sph-py-sulfosalt sulfides	X		X	X								X		X			X	Atoll intergrowths	98	90.3	1.35	1.06	16.8
36508	RMUG08-120	55.88	55.93	Py-aspy-tetra-cpy; Au-rich zone	X		X	X								X		X			X	Atoll intergrowths, free Au	17.2	240	2.27	4.35	5.21
36509	RMUG08-120	56.48	56.52	Py-aspy-tetra with black material in py-rich sulfide.	X		X	X			X		X			X		X			X	Sulfosalt atolls	25.9	670	4.86	3.78	6.12
36510	RMUG08-120	59.61	59.65	Py-aspy-cpy sulfide; py>>aspy,cpy	X		X	X			X					X		X			X		84.6	140	2.63	4.06	0.165
36511	RMUG08-120	60.22	60.25	Ga-sph-chl-rich sulfide	X			X			X		X			X		X			X		14.6	430	1.55	16.5	2.2
36512	RMUG08-123	59.48	59.53	Sph-ga-rich sulfide	X			X			X					X		X	X			Stannite present	90.4	907	3.14	1.83	2.68
36513	RMUG08-123	63.09	63.14	Py-cpy-rich sulfide; Au-rich zone	X		X	X			X		X			X					X	Atoll intergrowths with Au	72.8	431	2.9	8.18	1.47
36514	RMUG08-123	63.54	63.59	Py-sulfosalt-ga sulfides	X		X	X			X					X		X			X		72.8	431	2.9	8.18	1.47
36515	RMUG08-123	63.63	63.67	Cpy-py-aspy sulfide	X	X		X			X					X		X		X	X		14.7	49.5	0.533	0.741	0.063
36516	RMUG08-125	49.56	49.61	Ga-sph-cpy-rich sulfide with sulfosalts	X			X			X					X		X			X		28.7	303	2.31	4.44	5.1
36517	RMUG08-125	52.09	52.13	Py-sph-cpy-aspy sulfide	X		X	X			X					X		X			X		46	57	1.65	1.02	14
36518	RMUG08-128	54.26	54.29	Py-sph-aspy-cpy sulfide	X	X	X	X			X		X		X	X		X			X	Atoll intergrowths	28.3	396	1.92	4.31	19.7
36519	RMUG08-125	55.28	55.33	Py-aspy-tetra sulfide	X		X	X			X		X		X	X		X	X		X		15.4	195	0.714	3.43	2.01
36520	RMUG08-142	60.51	60.55	Grainy pyritic sulfide	X		X	X			X		X			X		X	X		X		21.498	295.3	2.39		7.5
36521	RMUG08-142	64.74	64.78	Cu-rich sulfide with sph, po, sulfosalts	X	X	X	X		?		X				X	X	X				Metamorphosed	8.243	130.4	3		1.9
36522	RMUG08-142	65.53	65.57	Buckshot sulfides with py-po-sph		X	X					X		X		X	X	X					20.675	222.5	9.1		1.18

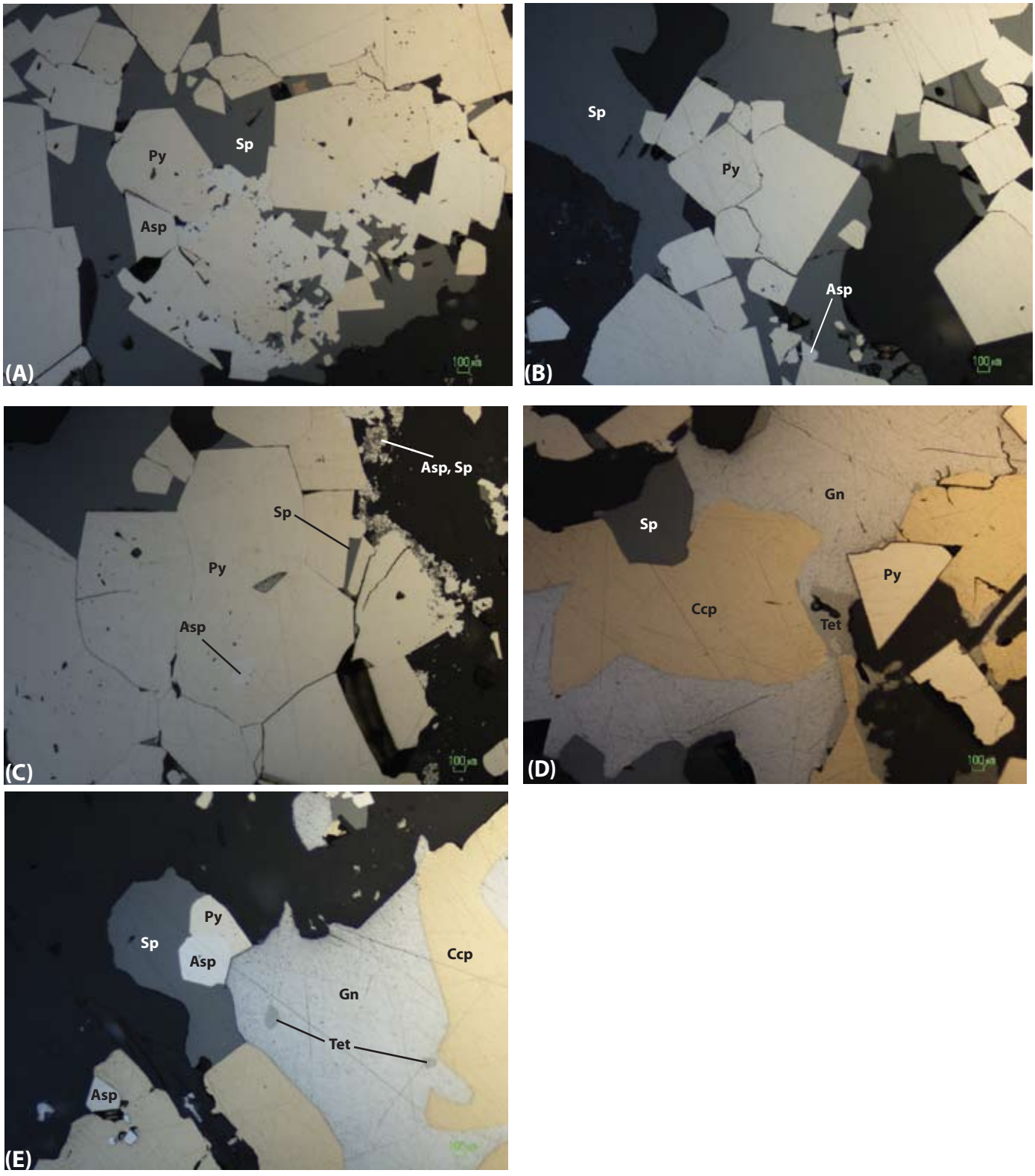

Figure 1. Sample 36501. A, B) Euhedral pyrite-arsenopyrite crystals with interstitial sphalerite. C) Annealed pyrite crysatls with intergrown arsenopyrite and sphalerite. Note the needlework of arsenopyrite crystals intergrown with sphalerite near the gangue in this photo. D) intergrowths of galena, chalcopyrite, and pyrite. Note tetrahedrite exsolution in the galena. E) Galena-chalcopyrite-sphalerite-pyrite-arsenopyrite assemblage with exsolved blebs of tetrahedrite in galena.

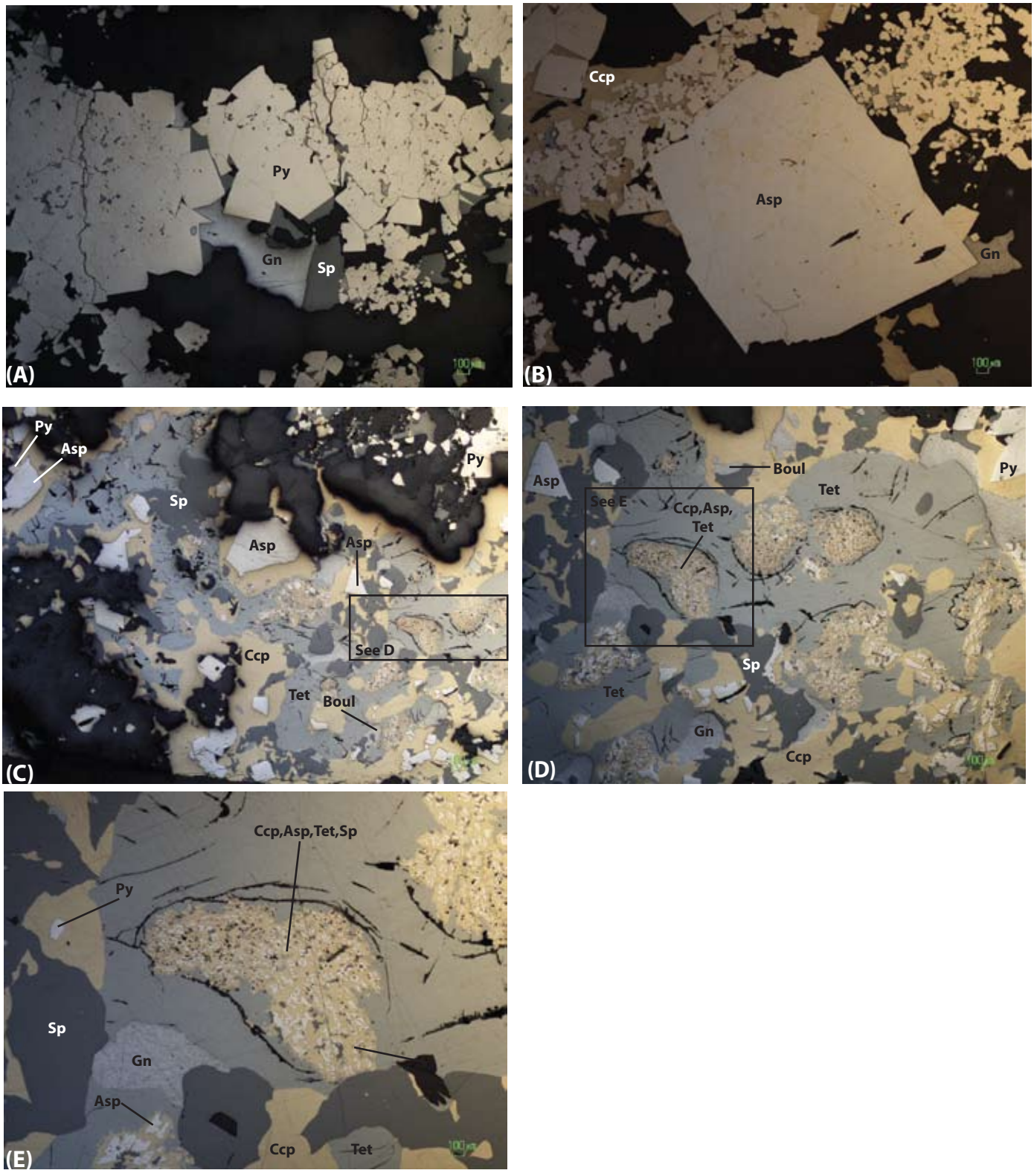

Figure 2. Sample 36502. A) Euhedral pyrite grains with variable annealing with interstitial anhedral galena and sphalerite. B) Arsenopyrite porphyroblast with inclusions of pyrite surrounded by chalcopyrite and smaller pyrite and arsenopyrite crystals. C, D, E) Typical sulfide-sulfosalt relationships with pyrite, arsenopyrite, sphalerite, tetrahedrite, boulangerite, galena, and chalcopyrite. Notably, there are well developed atolls that contain intergrowths of arsenopyrite needles with chalcopyrite, tetrahedrite, and sphalerite. These intergrowths have gold in other samples. Note the abundance of tetrahedrite intergrown with the chalcopyrite and other phases.

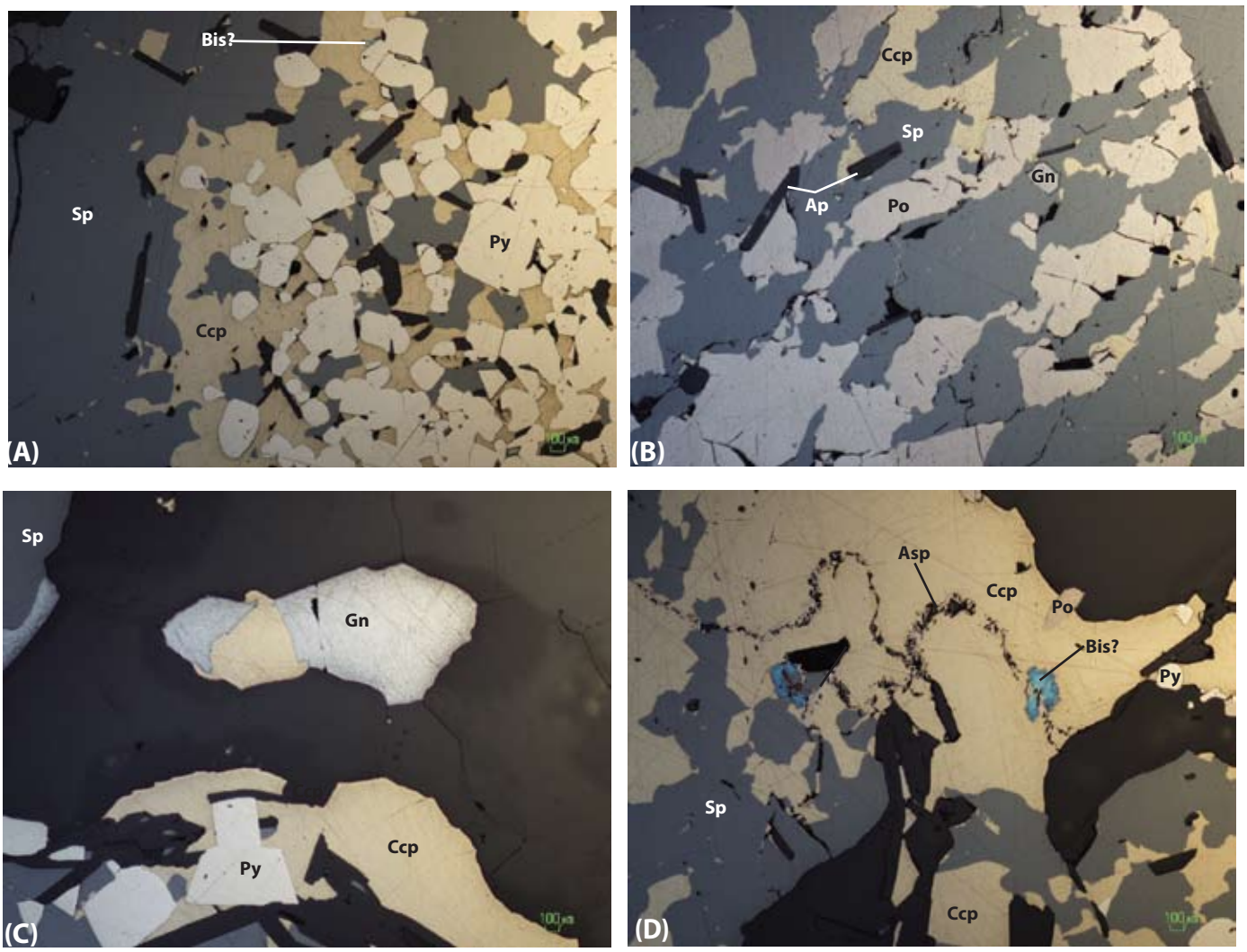

Figure 3. Sample 36503. A) Euhedral pyrite crystals intergrown with sphalerite and chalcopyrite. Bright blue, fibrous material in chalcopyrite is likely tarnished bismuthinite. B) Pyrrhotite-rich sulfides with chalcopyrite, sphalerite, galena, and apatite. C) Galena-chalcopyrite-pyrite-sphalerite-bearing sulfide assemblage. D) Chalcopyrite with sphalerite, pyrite, and a train of needles of arsenopyrite with tarnished bismuthinite.

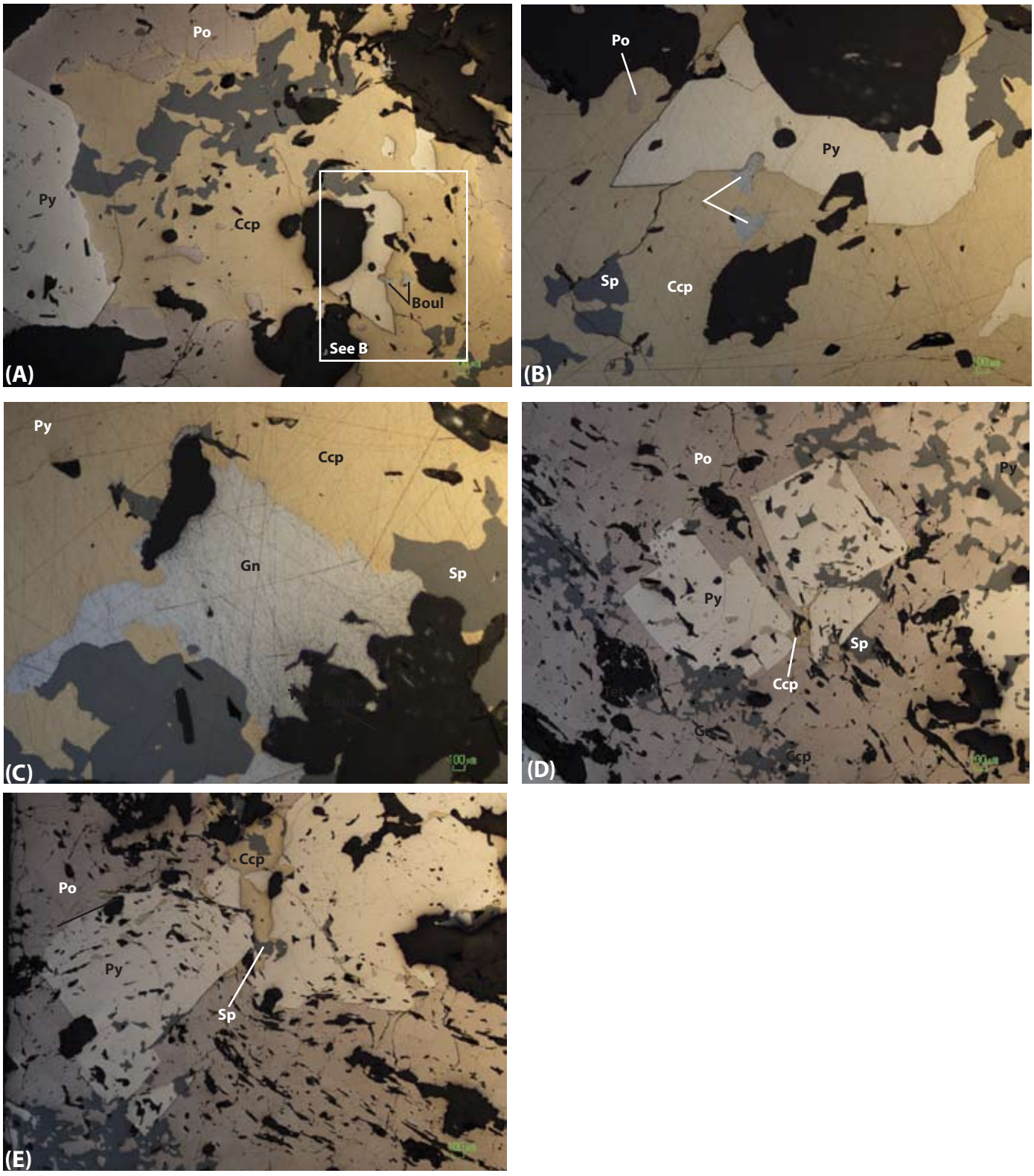

Figure 4. Sample 36504. A) Chalcopyrite-pyrrhotite-pyrite-sphalerite-boulangerite-bearing sulfides. B) Close up of (A). C) Galena within chalcopyrite with sphalerite. D) Pyrite porphyroblasts within a sea of pyrrhotite with sphalerite and chalcopyrite inclusions. E) Pyrite porphyroblasts within sea of pyrrhotite with porphryoblasts growing over the deformation fabric.

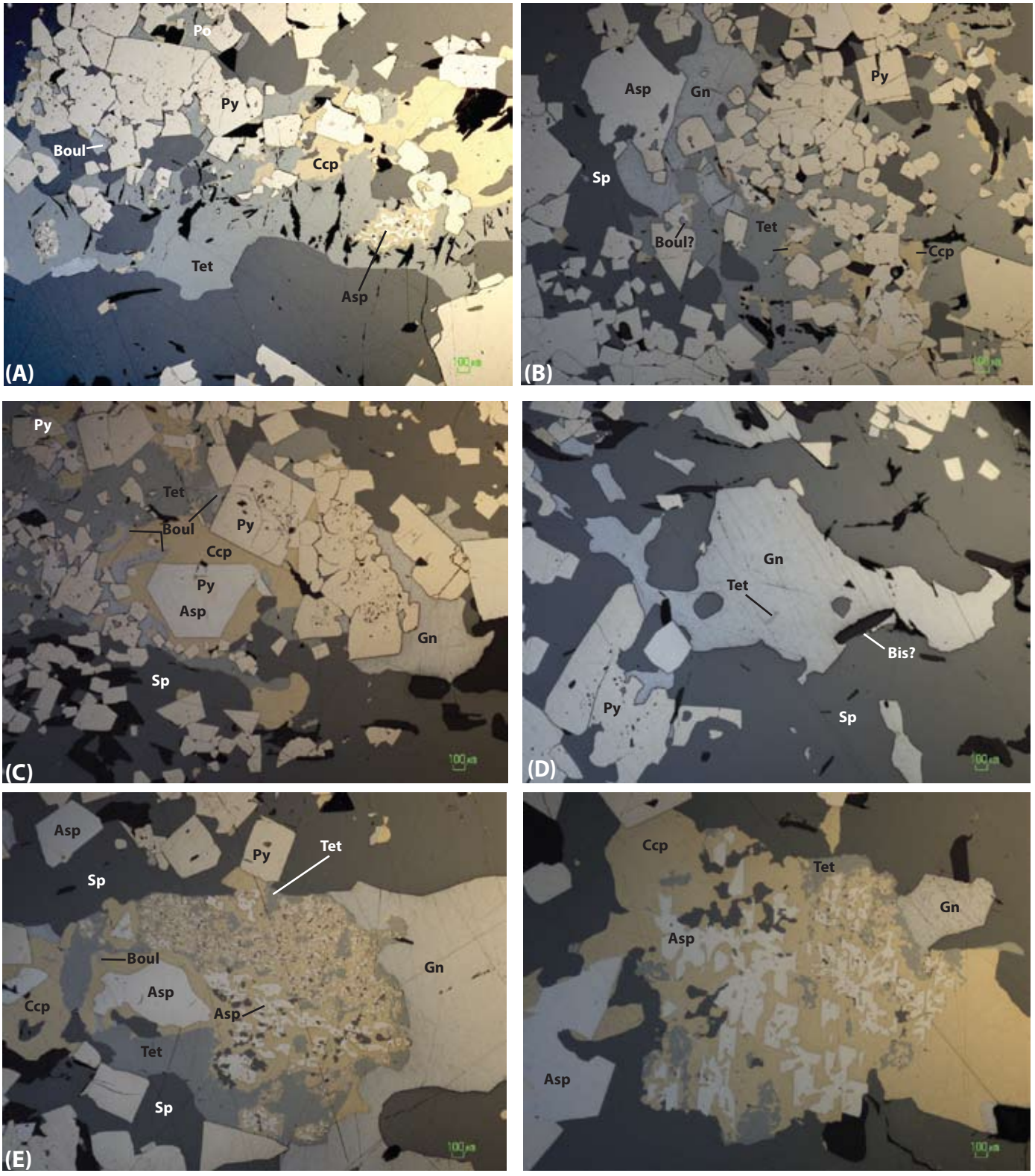

Figure 5. Sample 36505. A) Tetrahedrite-sphalerite-pyrite-chalcopyrite-bearing assemblage with chalcopyrite-arsenopyrite-tetrahedrite intergrowths in tetrahedrite. Note the polishing cleavage in the tetrahedrite. B) Pyrite-galena-tetrahedrite-arsenopyrite-chalcopyrite-boulangerite(?) assemblage. C) Euhedral pyrite and arsenopyrite grains with chalcopyrite, tetrahedrite, galena, sphalerite, and boulangerite. D) Pyrite and sphalerite with galena that has inclusions of tetrahedrite (exsolution blebs) and potential bismuthinite. E) Intergrowths of tetrahedrite-arsenopyrite needles-chalcopyrite within tetrahedrite and galena with arsenopyrite, sphalerite, and pyrite nearby. F) Close up of a chalcopyrite-tetrahedrite-arsenopyrite intergrowth with galena, sphalerite, pyrite, and larger arsenopyrite grains nearby. These intergrowths commonly host gold in the 1806 zone.

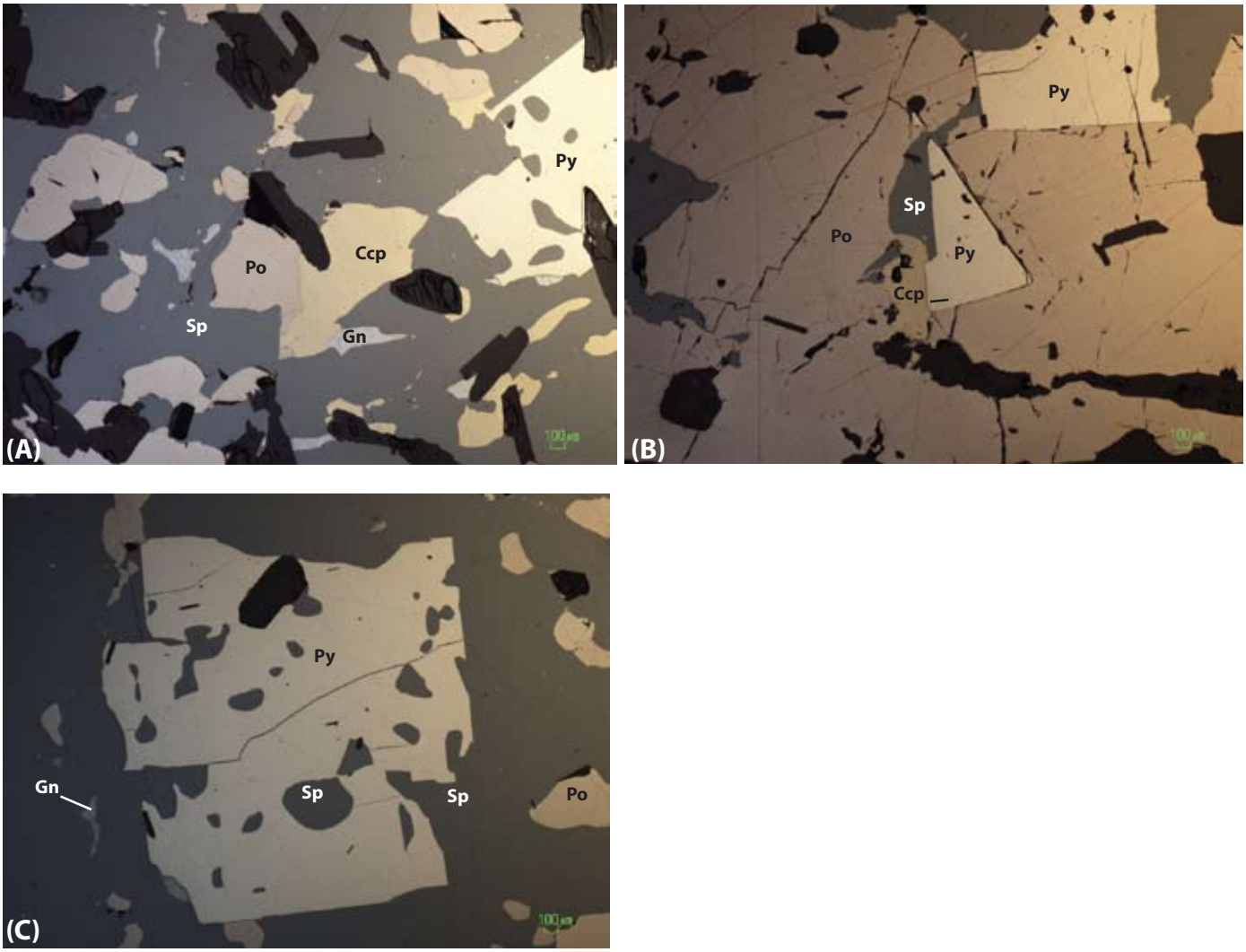

Figure 6. Sample 36506. A) Sphalerite-chalcopyrite-pyrrhotite-pyrite-galena-bearing assemblage. B) Pyrite grains with chalcopyrite and sphalerite within a pyrrhotite host crystal. C) Swiss cheese pyrite porphyroblast with sphalerite inclusions within a matrix of sphalerite with pyrrhotite and galena.

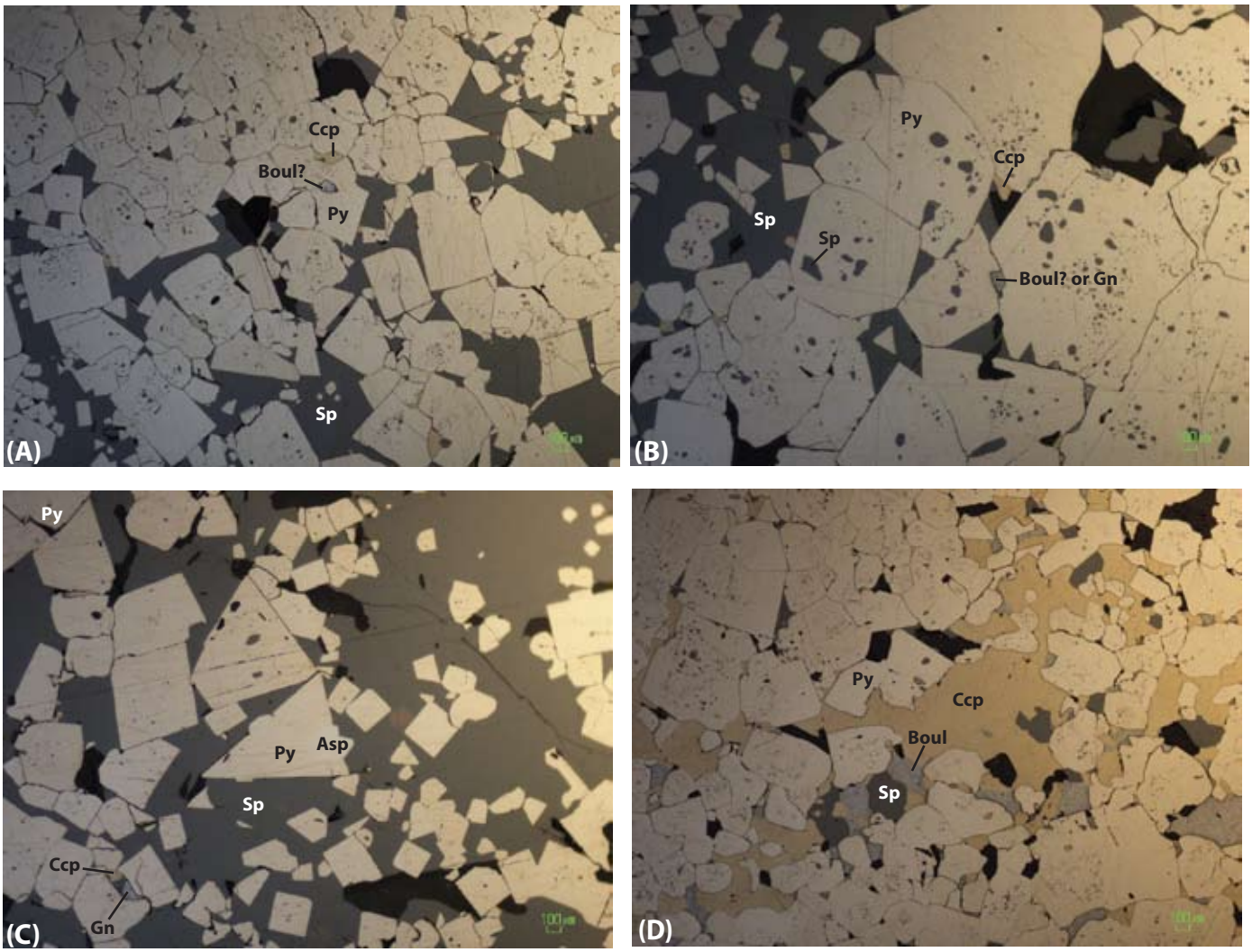

Figure 7. Sample 36507. A) Annealed pyrite with interstitital sphalerite, boulangerite, and chalcopyrite with inclusions of sphalerite and chalcopyrite. B) Close up of annealed pyrite with inclusions of sphalerite and chalcopyrite. C) Pyrite grains with arsenopyrite within sphalerite. D) Annealded pyrite with interstitial chalcopyrite, sphalerite, and boulangerite.

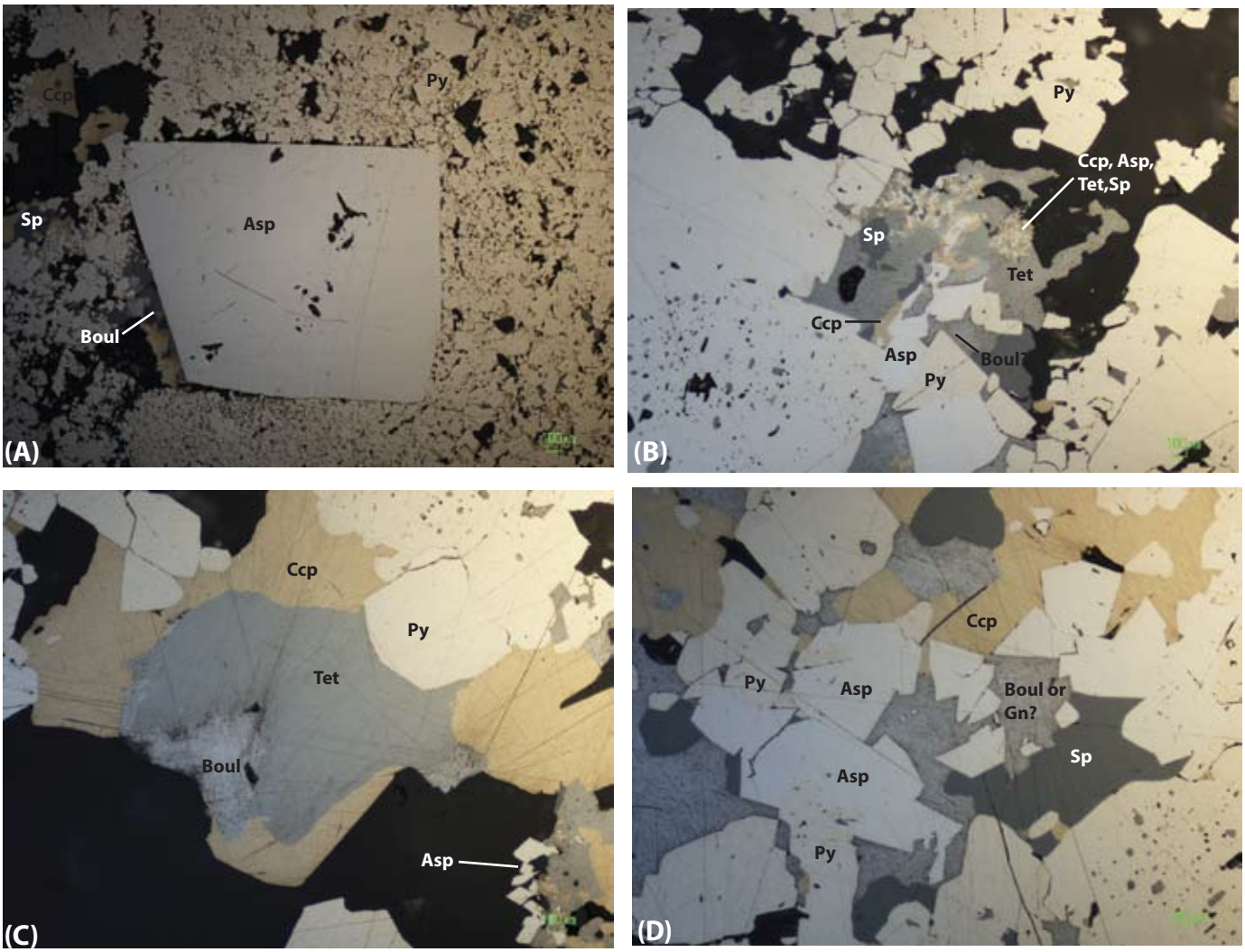

Figure 8. Sample 36508. A) Arsenopyrite porphyroblasts within a sea of annealed, euhedral pyrite with interstitial chalcopyrite, sphalerite, and boulangerite. B) Euhedral pyrite and arsenopyrite grains with irregular tetrahedrite-boulangerite-sphalerite-chalcopyrite-aresenopyrite intergrowths. Note the atolls of intergrown tetrahedrite-chalcopyrite-arsenopyrite-(sphalerite). C) tetrahedrite-chalcopyrite-pyrite-boulangerite assemblage. D) Euhedral pyrite and aresenopyrite with inerstitial boulangerite or galena, chalcopyrite, and sphalerite.

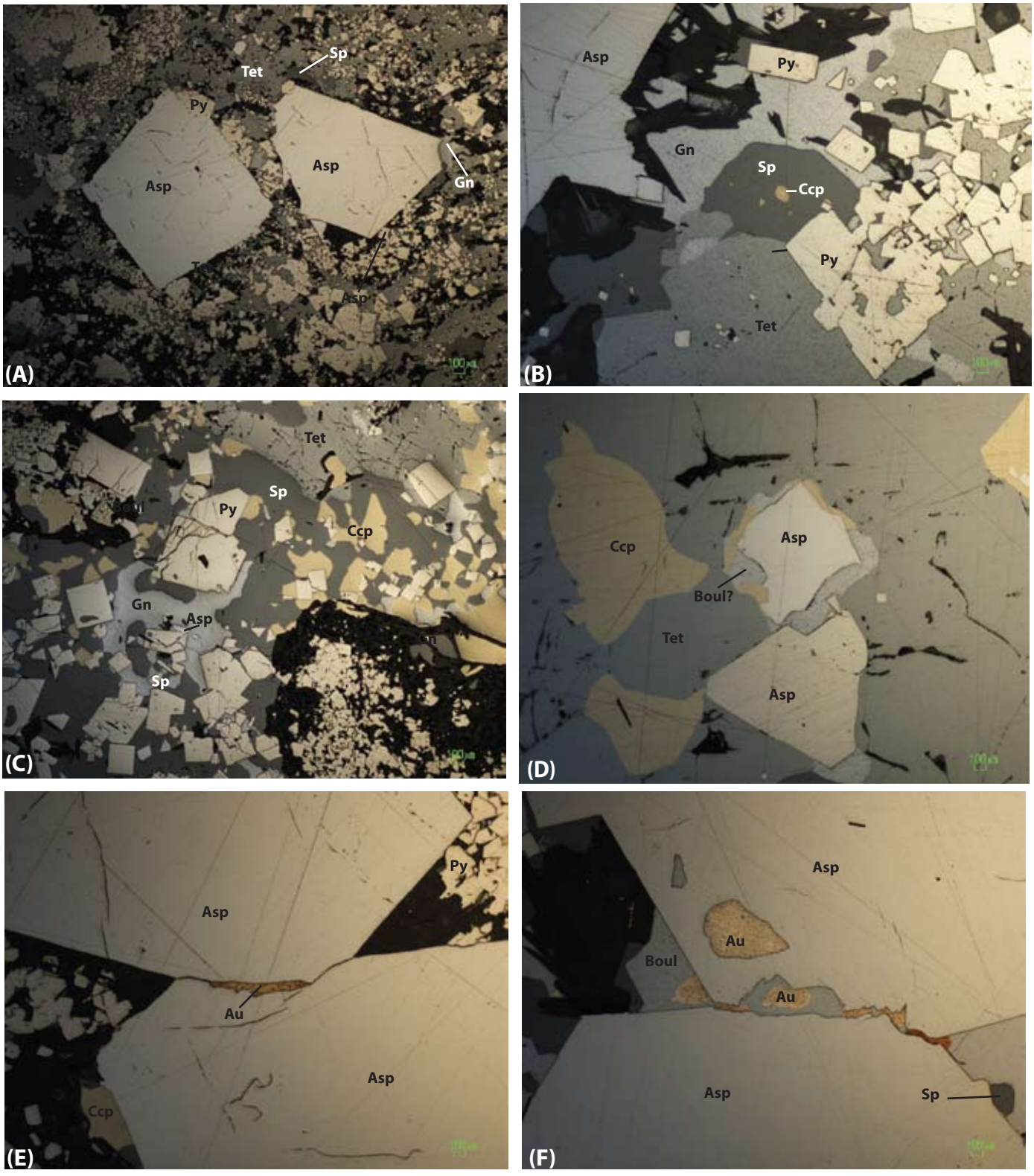

Figure 9. Sample 36509. A) Arseopyrite porphyroblasts with pyrite inclusions and pyrite along edges within a matrix of euhedral pyrite crystals with tetrahedrite, galena, and sphalerite. B) Pyrie-tetrahedrite-galena-arsenpyrite assemlbage. C) Sphalerite-tetrahedrite-chalcopyrite-galena-rich sulfides with eudhreal pyrite and arsenopyrite. D) Tetrahedrite host with chalcpyrite blebs, euhedral aresenopyrite crystals with boulangerite-chalcoyprite-intergrowths. E) Gold in between euhedral arsenopyrie crystals. F) Gold within arsenopyrite crystals and along arenopyite crystal edges inter-growth with boulangerite and sphalerite.

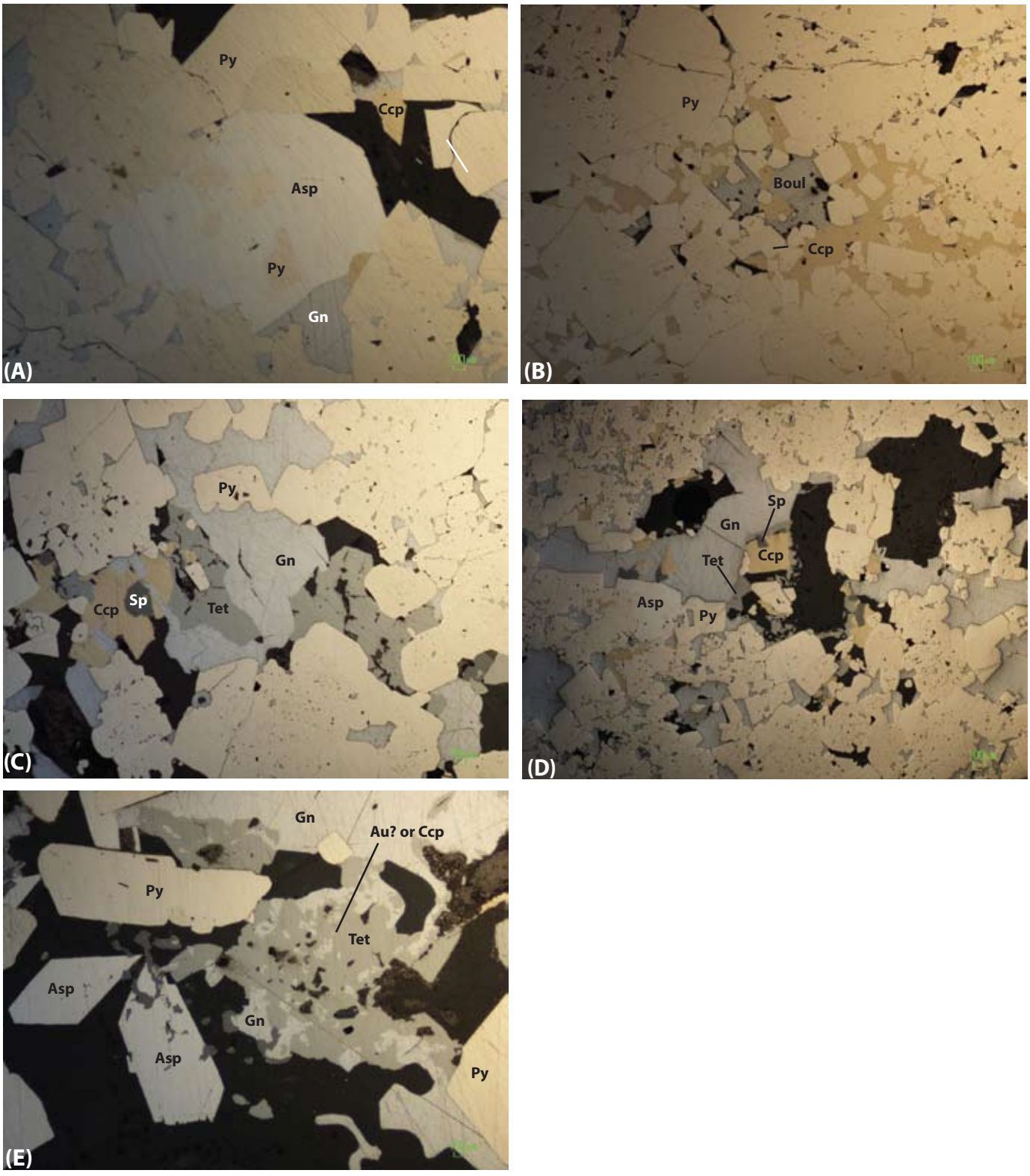

Figure 10. Sample 36510. A) Arseopyrite porphyroblasts with pyrite inclusions integrowth with annealed pyrite, chalcopyrite, and galena. B) Euhedral pyrite grains with interstitial chalcopyrite and boulangerite (note greenish hue to boulangerite). C) Pyrite-galena-tetrahedrite-sphalierite-chalcopyrite assemblage. D) Galena-pyrite rich sulfides with intergrown chalcopyrite-tetrahedrite-sphalerite. E) Euhedral arsenopyrite and pyrite crytsals near myrmekitically intergrown galena and tetrahedrite with a possible Au inclusion (or chalcopyrite).

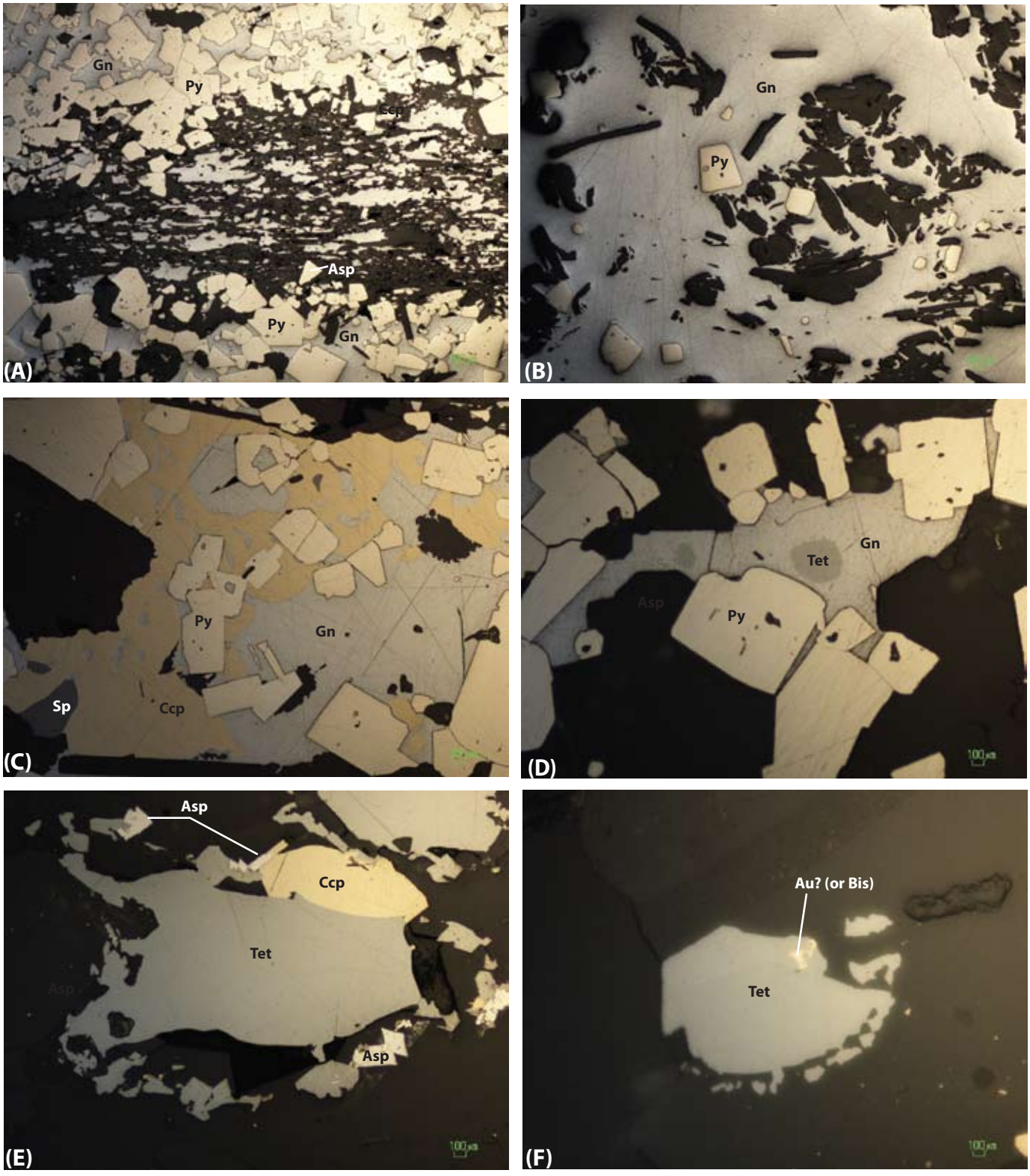

Figure 11. Sample 36511. A) Foliated sulfide sample with pyrite, galena, and aresenopyrite. B) Galena-rich sulfide with euhedral pyrite and chloritic gangue. C) Galena-chalcopyrite intergrown with euhedral pyrite and lesser anhedral sphalerite. D) Tetrahedrite-chalcopyrite-arsenopyrite intergrowths. E) Inclusion of Au (or bismuthinite) in tetrahedrite.

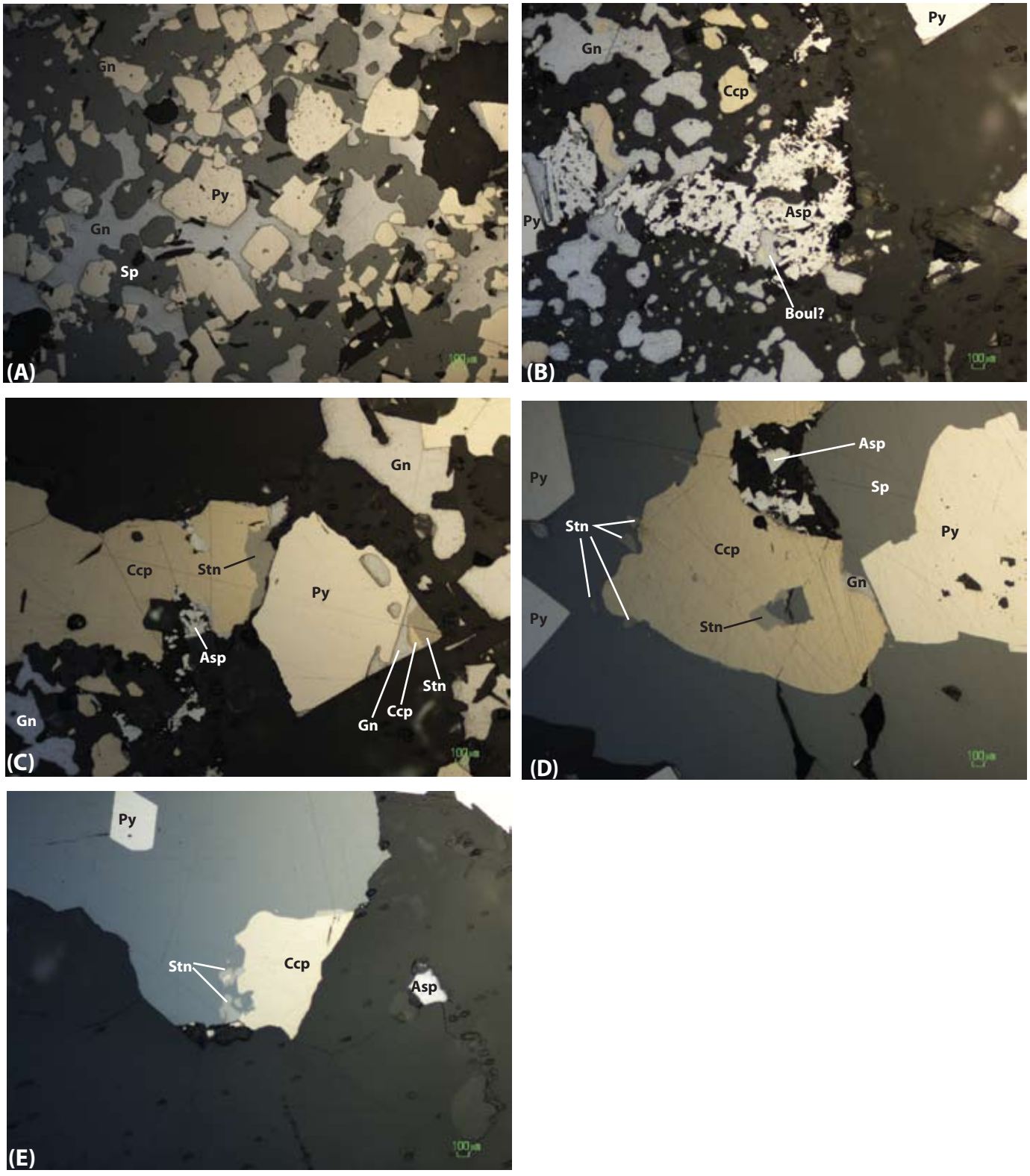

Figure 12. Sample 36512. A) Euhedral pyrite intergrown with sphalerite and galena. B) Arsenopyrite latticework of crystsals with galena, pyrite, chalcopyrite and boulangerite(?). C)Pyrite-galena-chalcopyrite-arsenopyrite-bearing assemblage with olive-brown crystals of stannite. D) Stannite blebs within and on the edges of chalcopyrite crystals. Other phases include pyrite, galena and sphalerite. E) Sphalerite with chalcopyrite crystals and pyrite inclusions with stannite blebs on the edge of the chalcopyrie crystals.

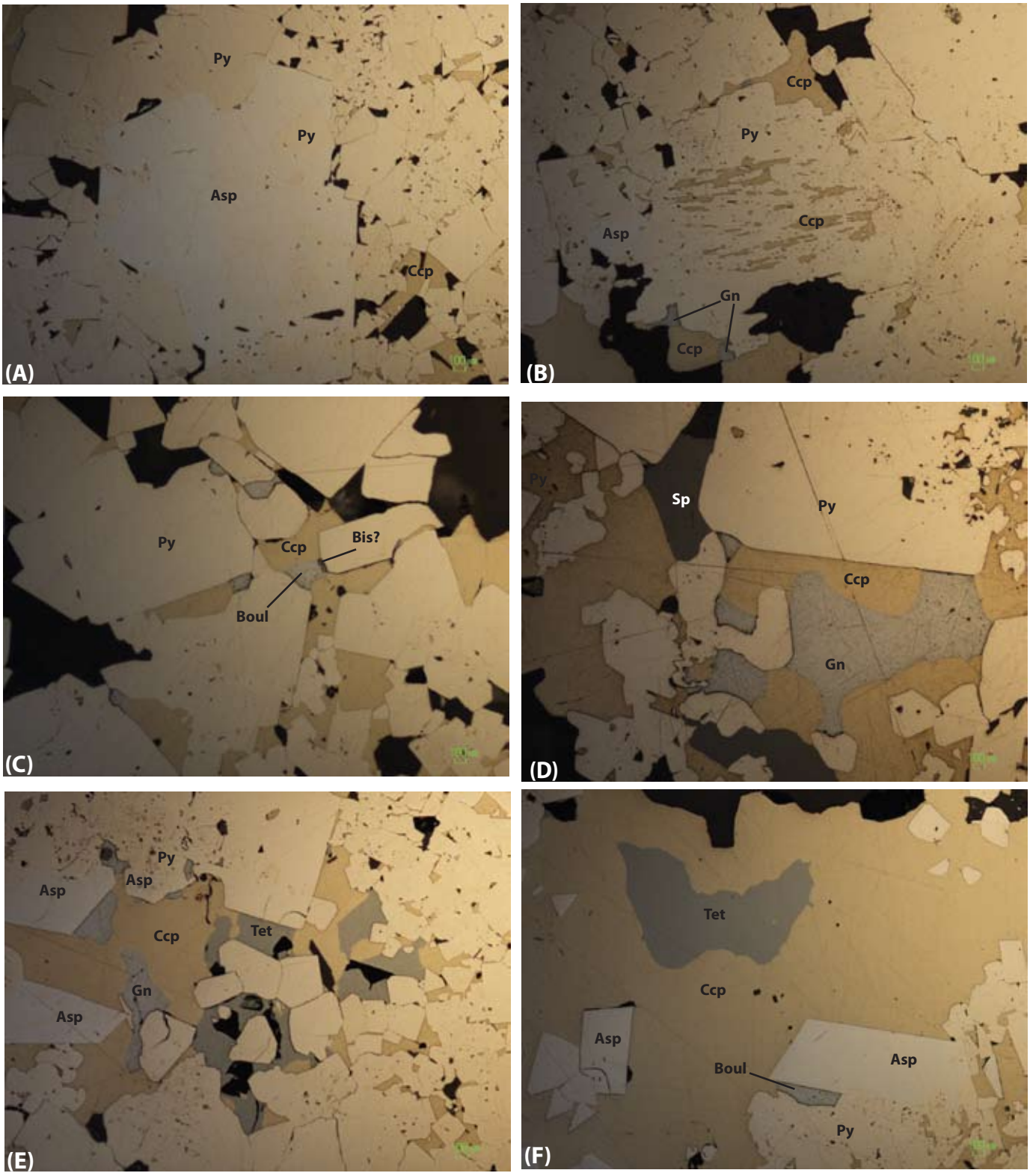

Figure 13. Sample 36513. A) Arsenopyrite porphyroblast with pyrite inclusions near euhedral pyrite with interstitial chalcopyrite. B) Pyrite crystals with latticework inclusions of chalcopyrite and interstitial chalcopyrite. C) Euhedral pyrite and arsenopyrite crystals with interstitial chalcopyrite and boulangerite (note greenish hue). D) Pyrite crystals with galena-chalcopyrite intergrowths. E) Euhedral pyrite and arsenopyrite with interstitial chalcopyrite, galena, and tetrahedrite. F) Chalcopyrite with euhedral inclusions of arsenopyrite and pyrite with lesser boulangerite.

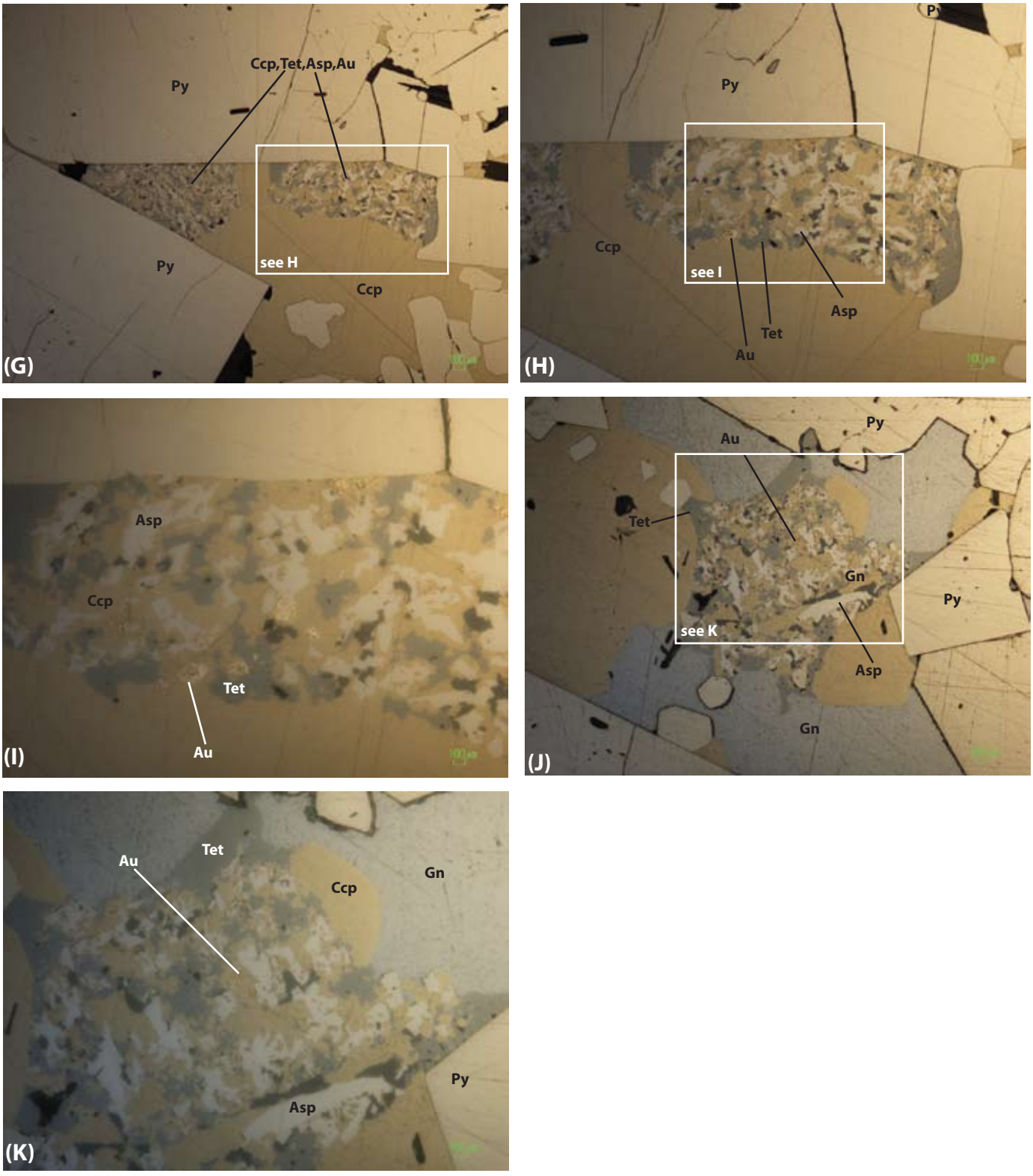

Figure 13 (continued). Sample 36513. G) Pyrite crystals with interstitial chalcopyrite and atoll-like intergrowths of chalcopyrite, arsenopyrite, tetrahedrite, and Au. H, I) close up of atolls in (G) with intergrown arsenopyrite, tetrahedrite, chalcopyrite and gold. J) Star shaped atoll intergrowth with galena, chalcopyrite, and pyrite nearby. Intergrowth consists of arsenopyrite-tetrahedrite-chalcopyrite-Au. K) close up of intergrowth in (J).

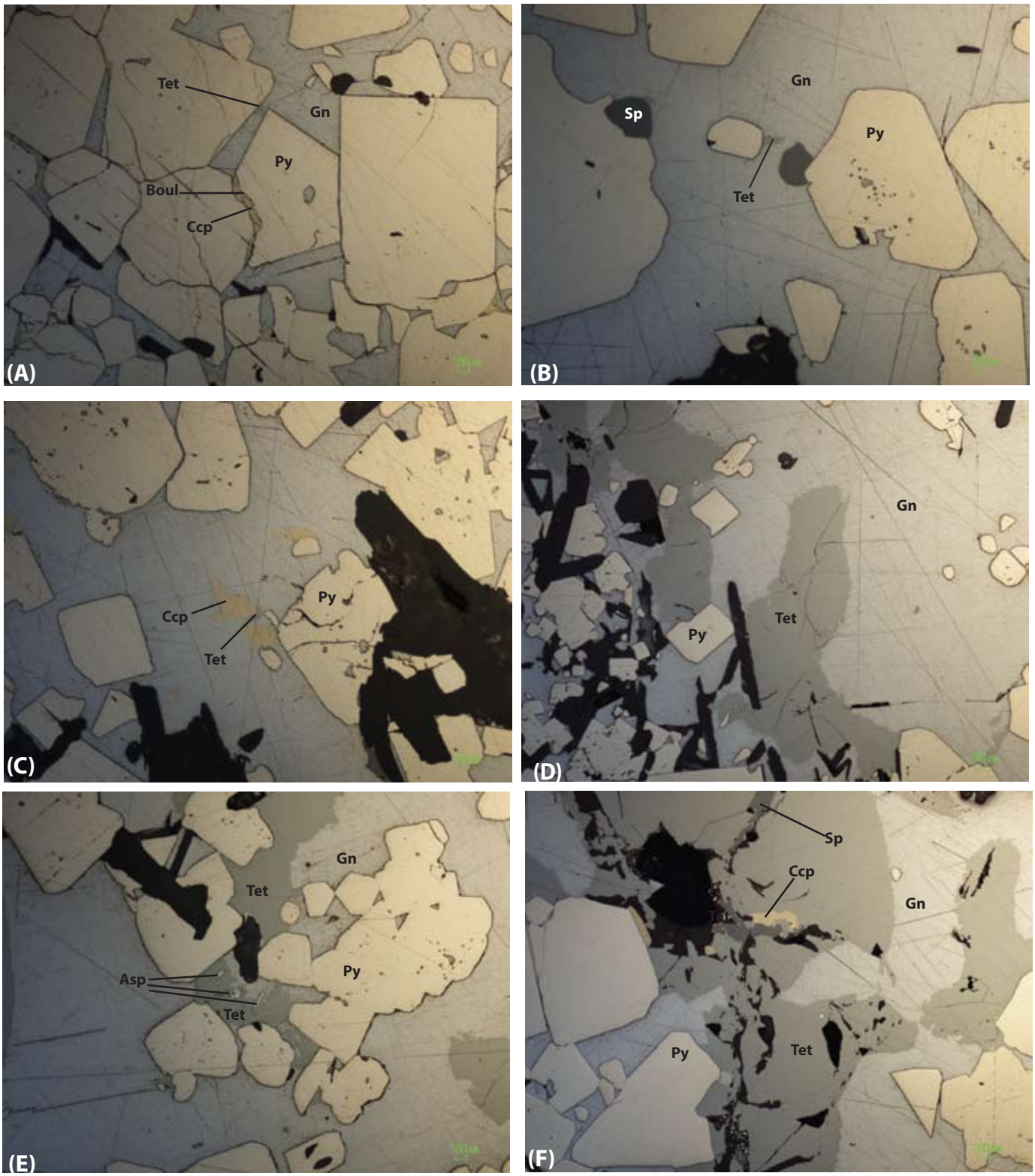

Figure 14. Sample 36514. A) Euhedral pyrite crystals with interstitial galena. Minor chalcopyrite and boulangerite are intergrown together. B) Galena with flames of tetrahedrite, euhedral to subhedral pyrite crystals, and sphalerite inclusions. C) Galena with chalcopyrite, pyrite, and tetrahedrite. D) Galena-tetrahedrite-rich sulfides with pyrite. E) Galena with tetrahedrite and pyrite. Needles of arsenopyrite are present within the tetrahedrite. F) Tetrahedrite-rich sulfides with galena, pyrite, chalcopyrite and sphalerite.

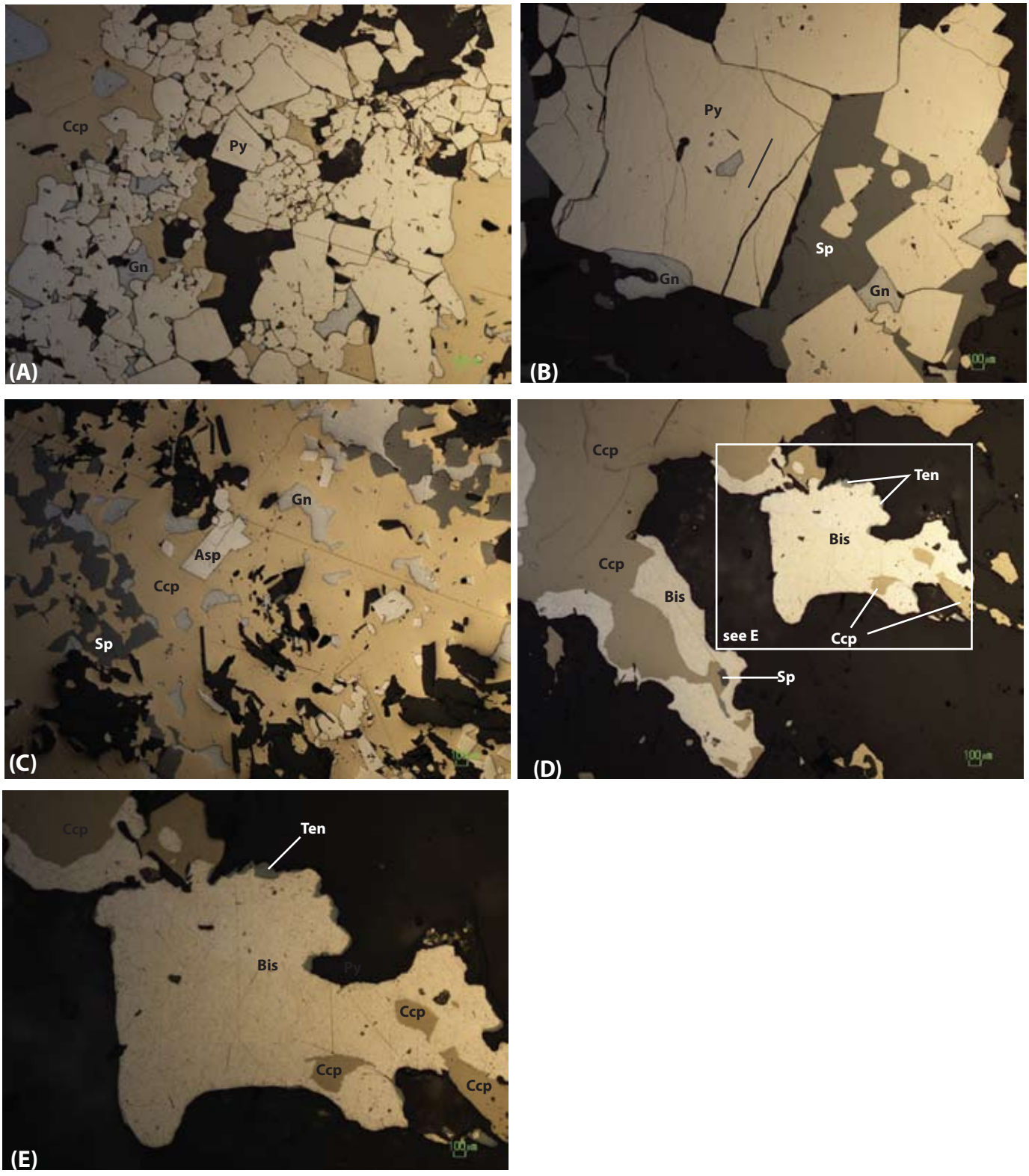

Figure 15. Sample 36515. A) Euhedral pyrite crystals with interstitial chalcopyrite and galena. B) Large, euhedral grains of pyrie with inclusions of galena and interstial galena and sphalerite. C) Chalcopyrite-rich sulfides with intergrown galena, sphalerite, and euhedral grains of arsenopyrite. D) Chalcopyrite with bismuthinite crystals along its edge. Riming the bismuthinite crystals is tennantite. E) Close up of (D) with bismuthinite with tennantite rims and inclusions of chalcopyrite.

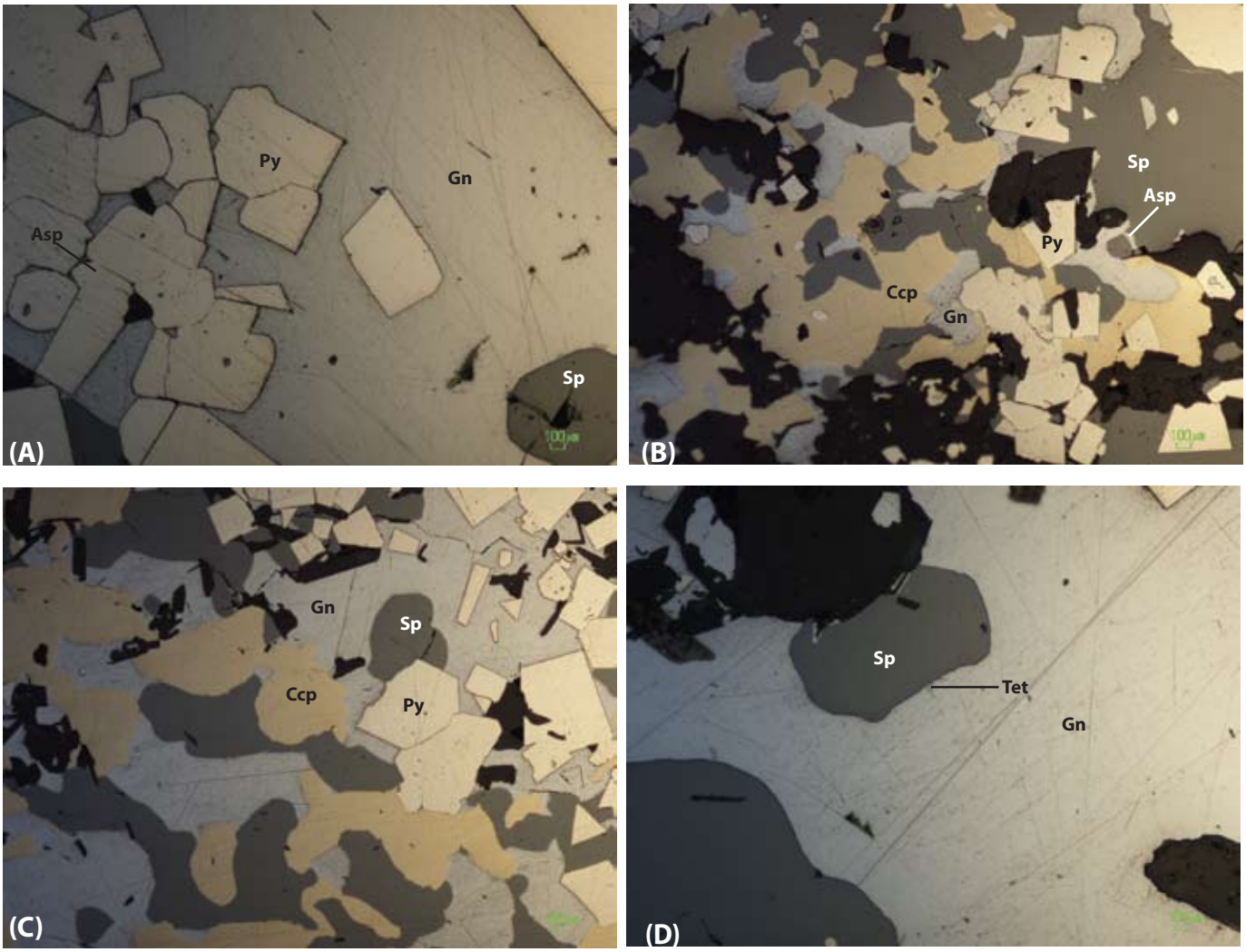

Figure 16. Sample 36516. A) Euhedral pyrite and anhedral sphalerite within galena. B) Euehdral pyrite with lesser arsenopyrite intergrown with chalcopyrite, galena, and sphalerite. C) Galena-sphalerite-chalcopyrite-pyrite assemblage. D) Galena with sphalerite and exsolution blebs of tetrahedrite.

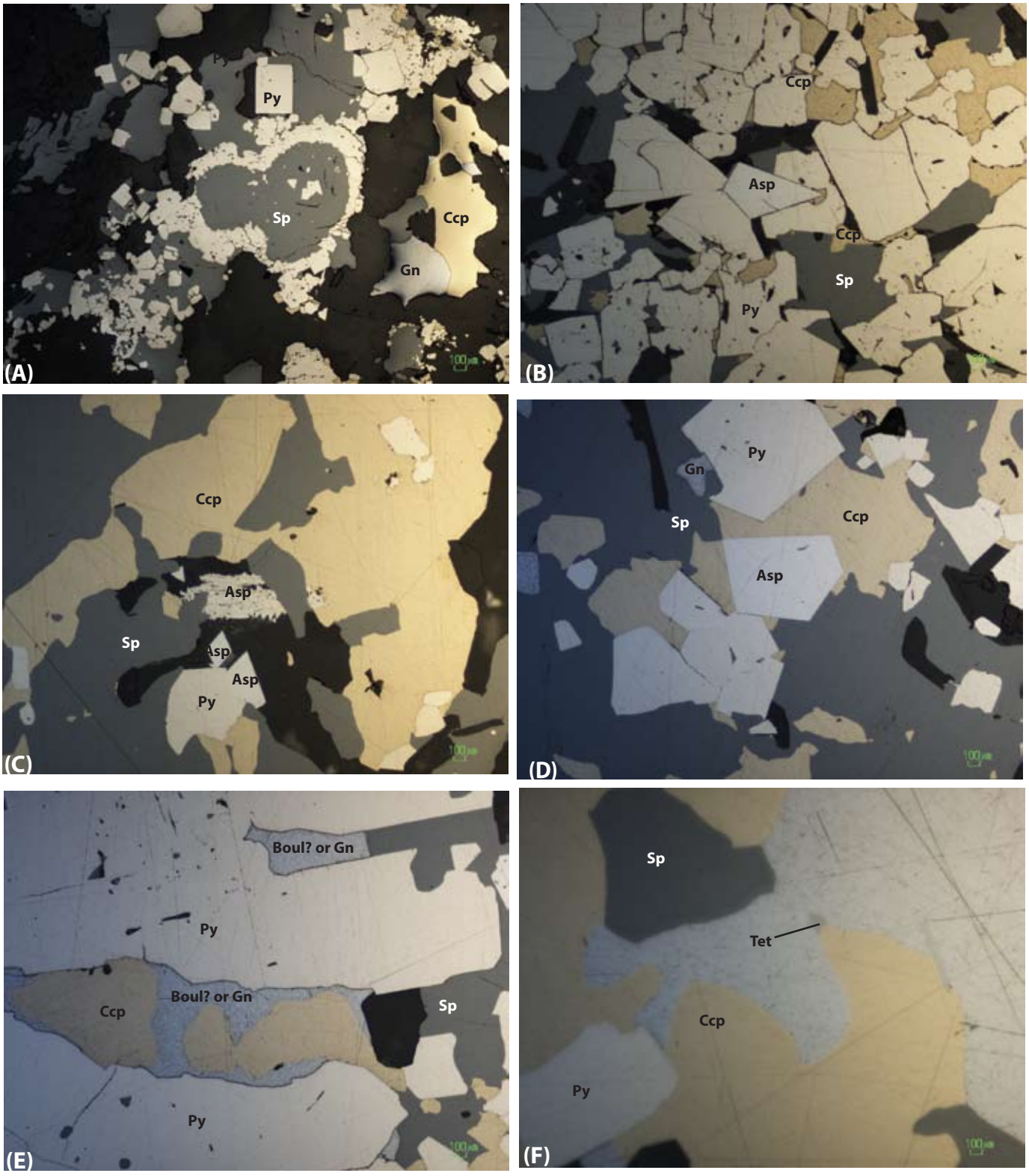

Figure 17. Sample 36517. A) Sphalerite surrounded by crystals of pyrite with nearby chalcopyrite and galena. B) Euhedral, annealed pyrite with arsenopyrite and interstitial sphalerite and chalcopyrite. C) Sphalerite-chalcopyrite-rich sulfides with latticework arsenopyrite aggregates and diamond-shaped arsenopyrite with pyrite. D) Arsenopyrite crystals with pyrite, sphalerite and chalcopyrite. E) Chalcopyrite with boulangerite (or galena) in between pyrite grains with sphalerite. F) Chalcopyrite, pyrite, sphalerite, and galena with tetrahedrite blebs in galena.

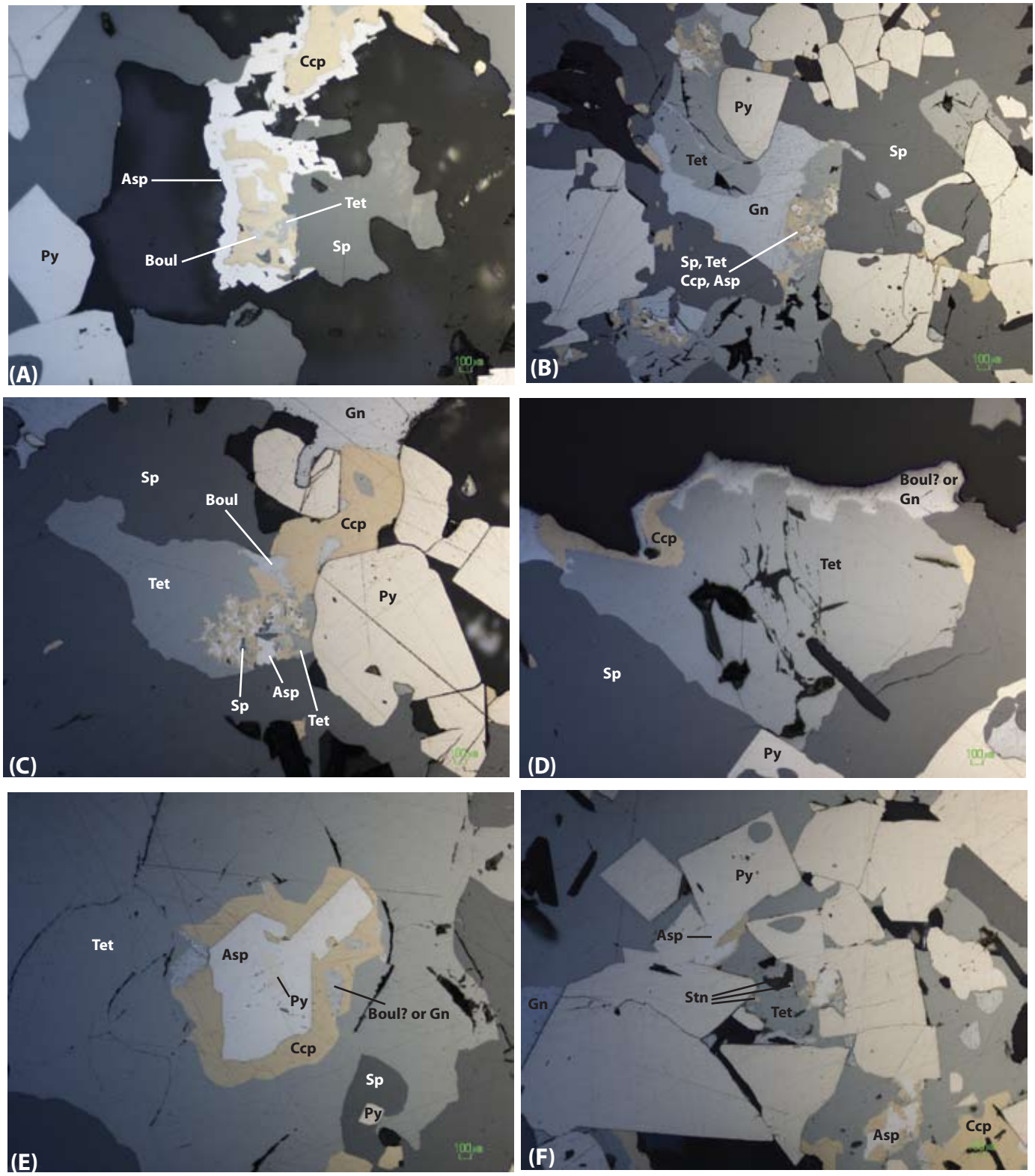

Figure 18. Sample 36518. A) Sphalerite-pyrite with chalcopyrite surrounded by a needlework of arsenopyrite crystals and with inclusions of tetrahedrite and boulangerite. B) Tetrahedrite-galena-pyrite-sphalerite-rich sulfides with atoll-like structures of sphalerite-tetrahedrite-chdalcopyrite-arsenopyrite intergrown with one another. C) Sphalerite-tetrahedrite-pyrite-chalcopyrite with atolls of sphalerite-arsenopyrite-pyrite-chalcopyrite intergrown witn one another. D) tetrahedrtie in sphalerite with a rim of chalcopyrite and boulangerite or galena. E) Arsenopyrite grain with pyrite inclusions surrounded by chalcopyrite with boulangerite or galena and hosted by tetrahedrite. F) Euhedral pyrite and arsenopyrite with interstitial galena and tetrahedrite and intergrowths of chalcopyrite, tetrahedrite, and arsenopyrite.

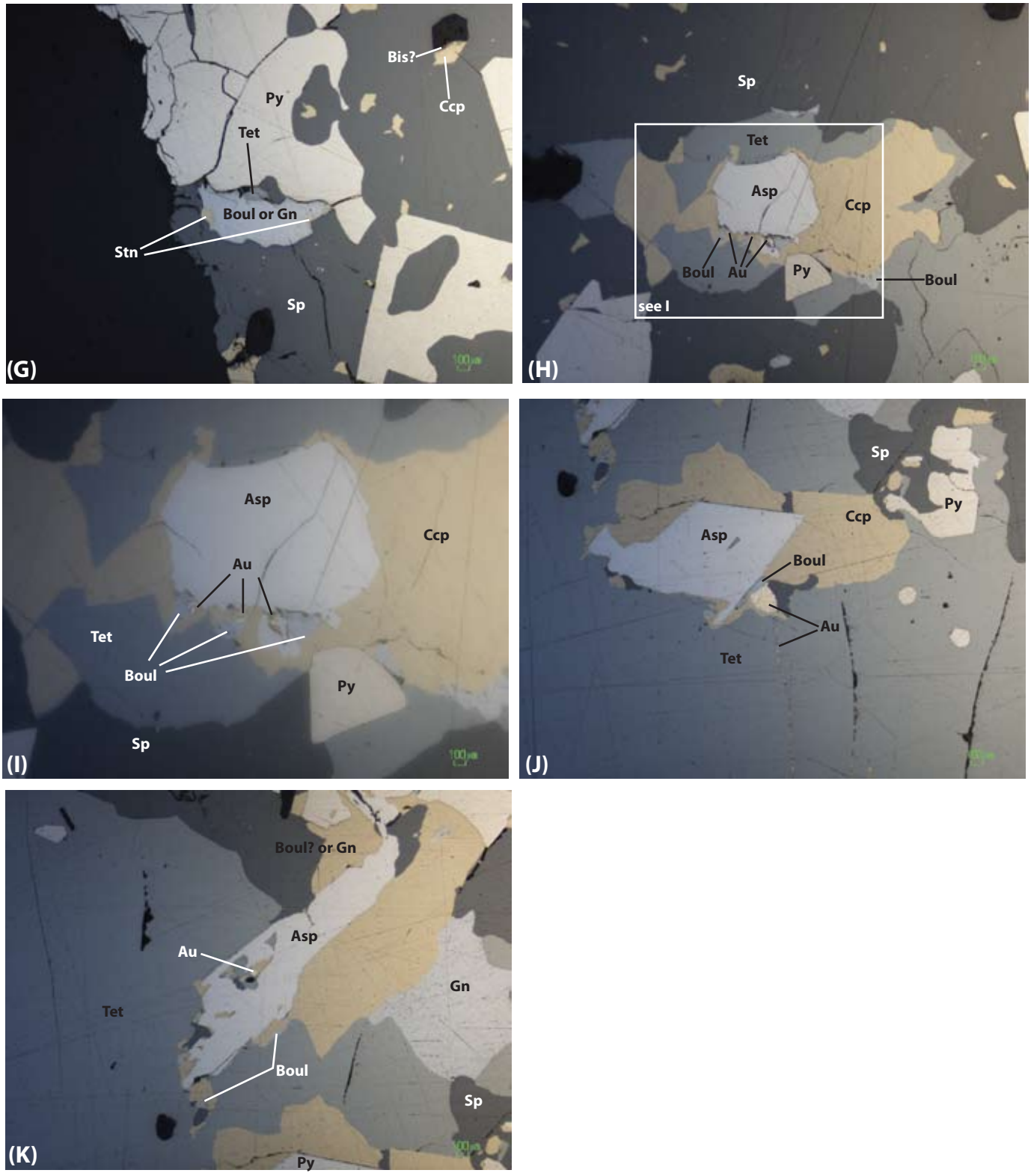

Figure 18 continued. Sample 36518. G) Sphalerite with pyrite and boulangerite crystal with stannite blebs. H) Tetrahedrite-chalcopyrite-arsenopyrite-sphalerite intergrowth with Au spatially associated with boulangerite. I) Close up of (H) illustrating the relationship of Au to boulangerite, arsenopyrite, chalcopyrite and tetrahedrite. J) Aresnopyrite grain hosted in chalcopyrite with tetrahedrite ang Au-boulangerite-sphalerite. K) Aresenopyrite crystal with inclusions of tetrahedrite, boulangerite, sphalerite and Au within a tetrahedrite-chalcopyrite assemblage. Galena is also present.

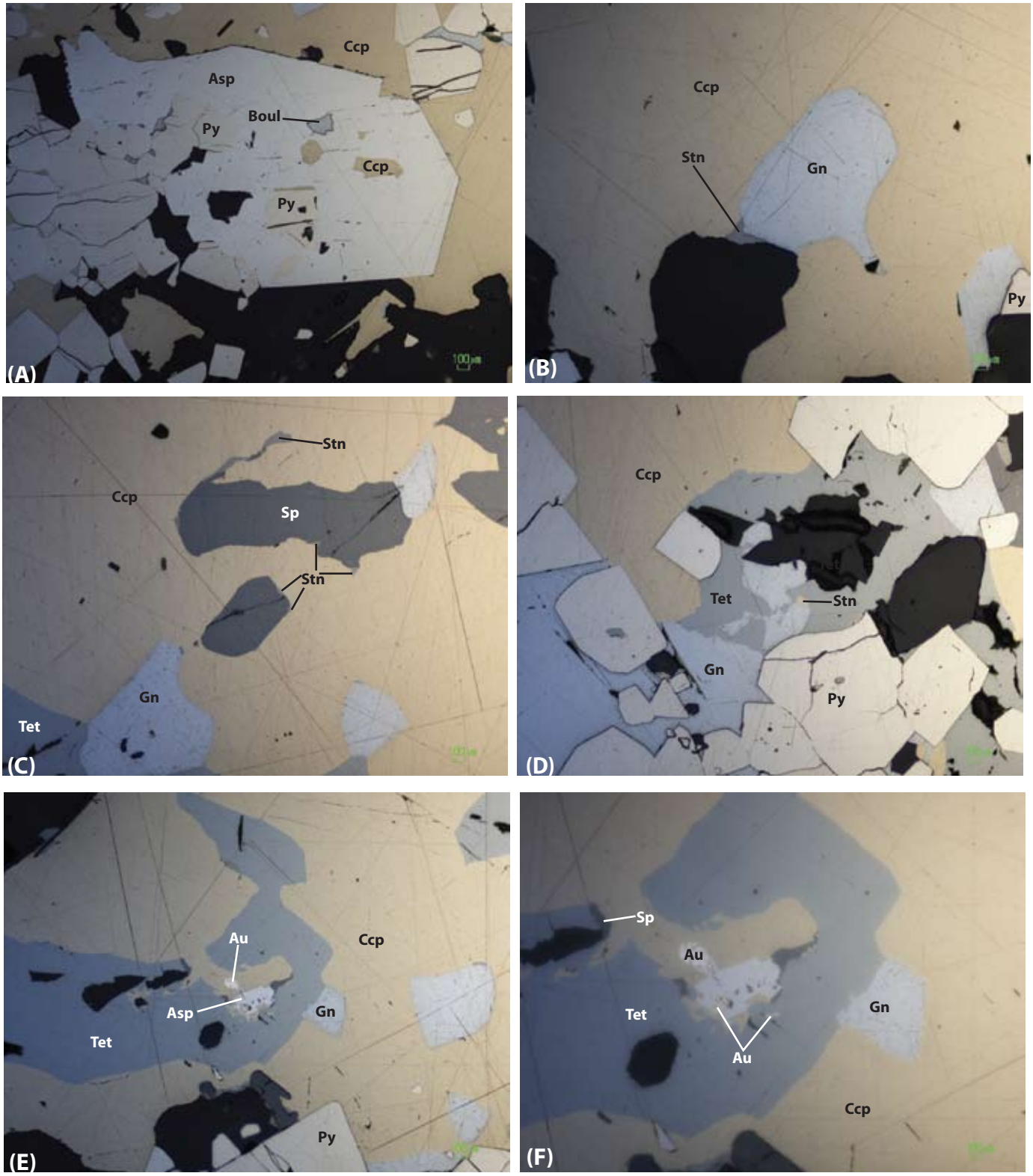

Figure 19. Sample 36519. A) Arsenopyrite grain with inclusions of pyrite, chalcopyrite, and boulangerite surrounded by chalcopyrite. B) Close up of chalcopyrite with galena and olive-brown stannite crystals. C) Chalcopyrite containing galena and sphalerite with chalcopyrite disease and blebs of stannite along sphalerite grain margins. D) Galena-tetrahedrite intergrowths with a stannite bleb near euhedral pyrite and anhedral chalcopyrite. E) Tetrahedrite, galena, and pyrite within chalcopyrite with arsenopyrite grains with gold near the aresenopyrite-tetrahedrite-chalcopyrite boundaries. F) Close up of (E) illustrate gold proximal to the arsenopyrite, tetrahedrite and chalcopyrite.

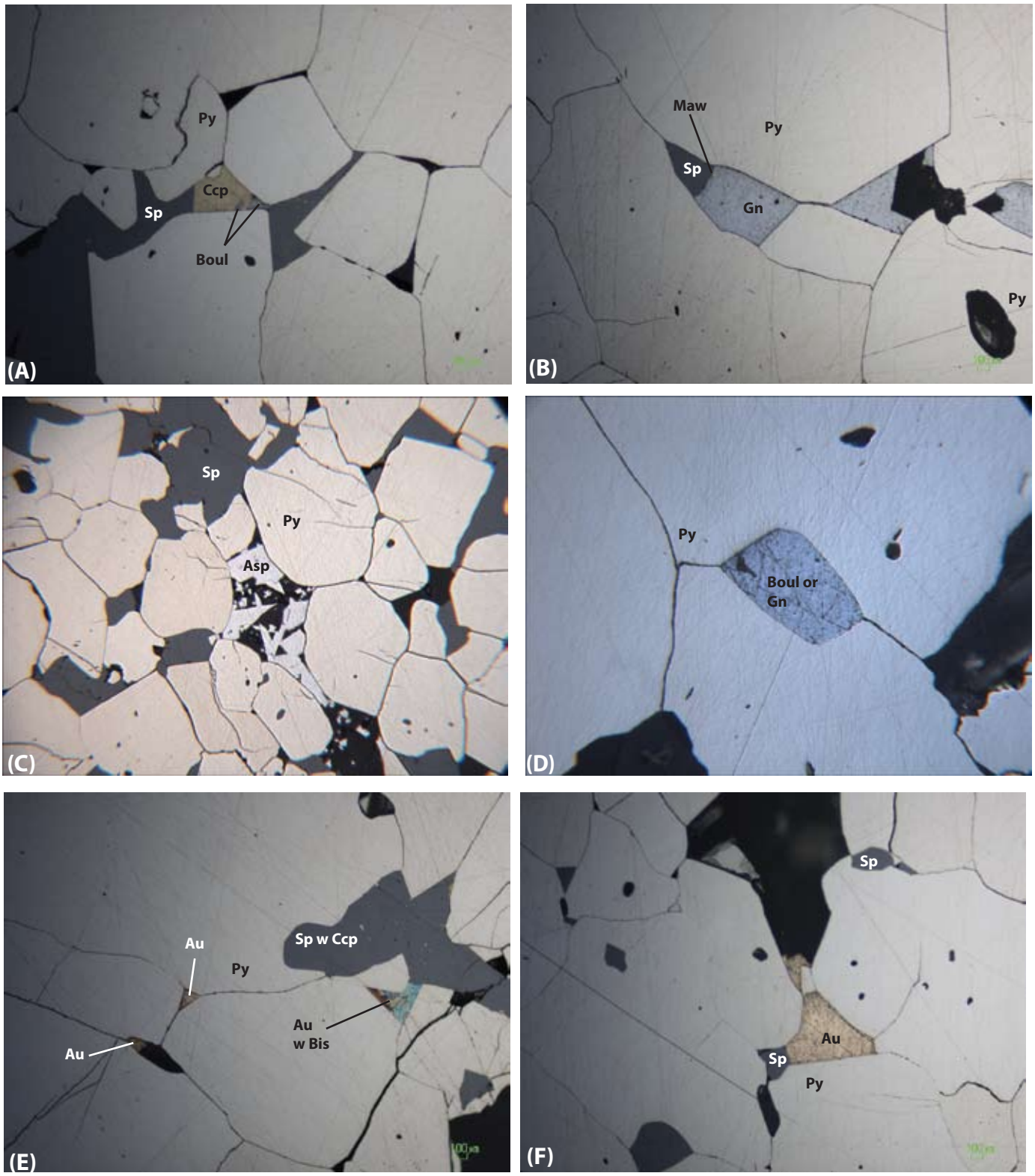

Figure 20. Sample 36520. A) Euhedral pyrite grains with interstitial sphalerite and chalcopyrite with boulangerite blebs. B) Annealed, euhedral pyrite with well developed triple junctions with intergrain galena and sphalerite. An orange-pink grain in galena is likely mawsonite. C) Euhedral pyrite grains with interstitial sphalerite and arsenopyrite needles (fiield of view: 900 microns). D) Euhedral and annealed pyrite with well developed triple junctions wiht interstitial boulangerite or galena (field of view: 180 microns). E) Annealed pyrite with interstitial sphalerite with chalcopyrite disease and interstitial Au and Au-bismuthinite intergrowth. Note the irridesence of bismuthinite in this photo. F) Pyrite grains with sphalerite inclusions and inter-grain Au and sphalerite.

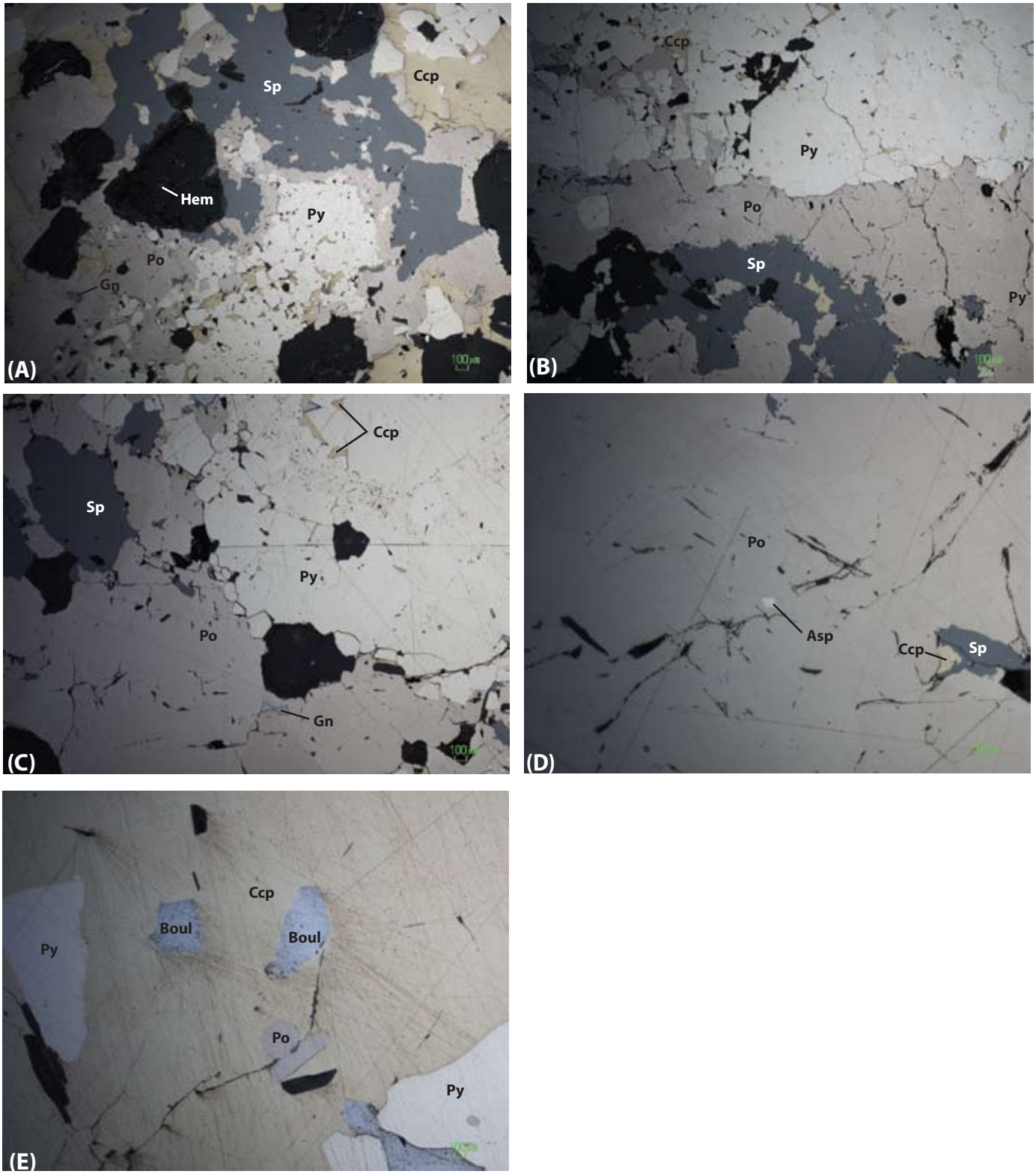

Figure 21. Sample 36521. A) Sphalerite-pyite-chalcopyrite-porrhotite-beaing sulfides with hematite associated with gangue phases. B) Pyrite-pyrrhotite-sphalerite-chalcopyrite-sulfides. C) Pyrite-pyrrhotite-galena-sphalerite-chalcopyrite-bearing sulfides. Note multiple growth zones in pyrite mass. D) Pyrrhotite with inclusion of arsenopyrite and sphalerite-chalcopyrite. E) Chalcopyrite with inclusions of boulangerite, euhedral pyrite, and pyrrhotite.

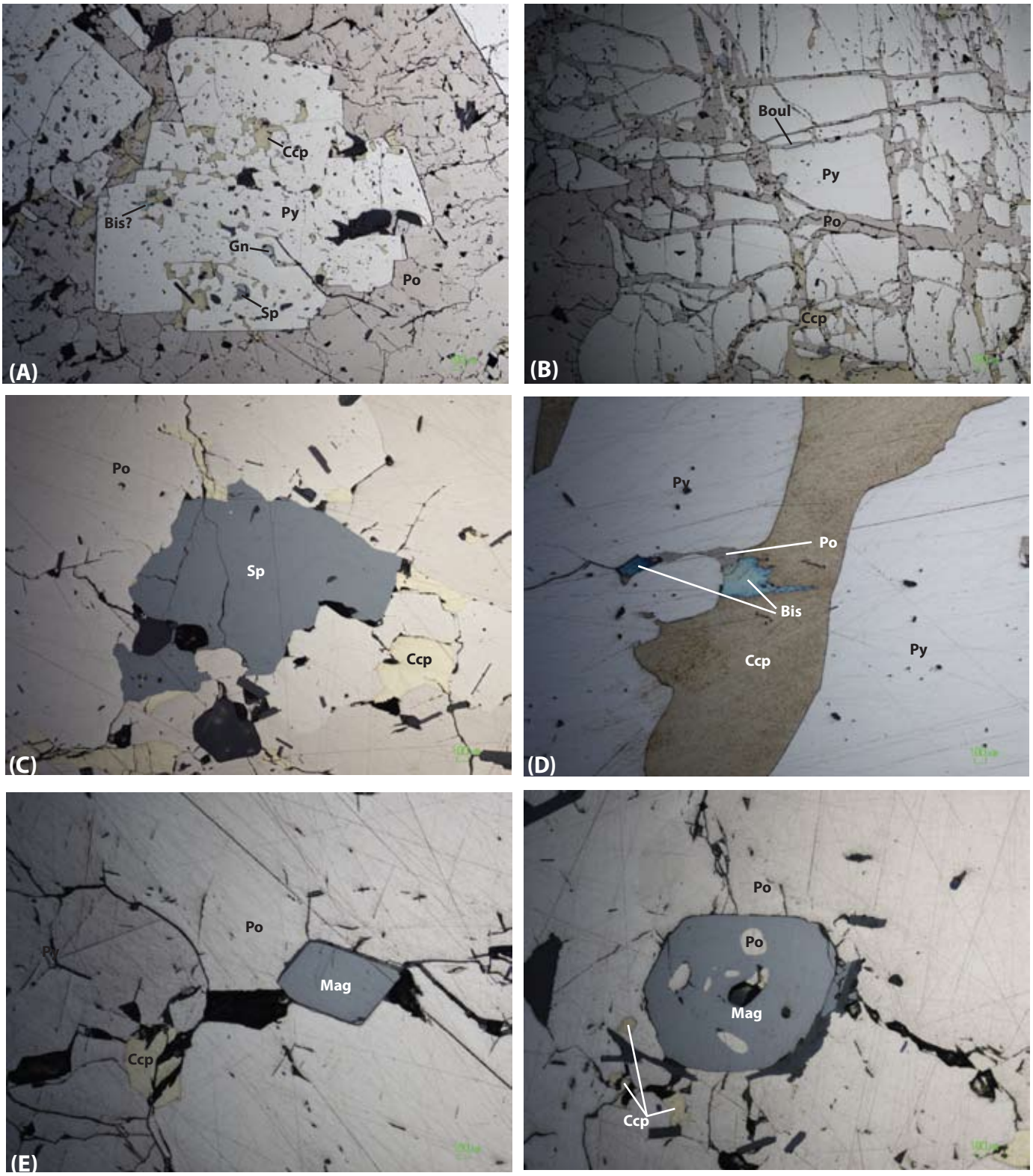

Figure 22. Sample 36522. A) Pyrite porphyroblast with inclusions of sphalerite, galena, chalcopyrite, and bismuthinite (note the absence of pyrrhotite, which is a rare phase in the pyrite buckshot grains). B) Pyrite porphyroblast with cracks filled with pyrrhotite, chalcopyrite, and boulangerite. C) Sphalerite grains in between pyrrhotite grains; chalcopyrite is also present. D) Pyrite grains with interstitial chalcopyrite and irridescent bismuthinite near pyrrhotite. E) Magnetite crystal associated with pyrrhotite and chalcopyrite. F) Magnetite crystal in pyrrhotite with inclusions of pyrrhotite.

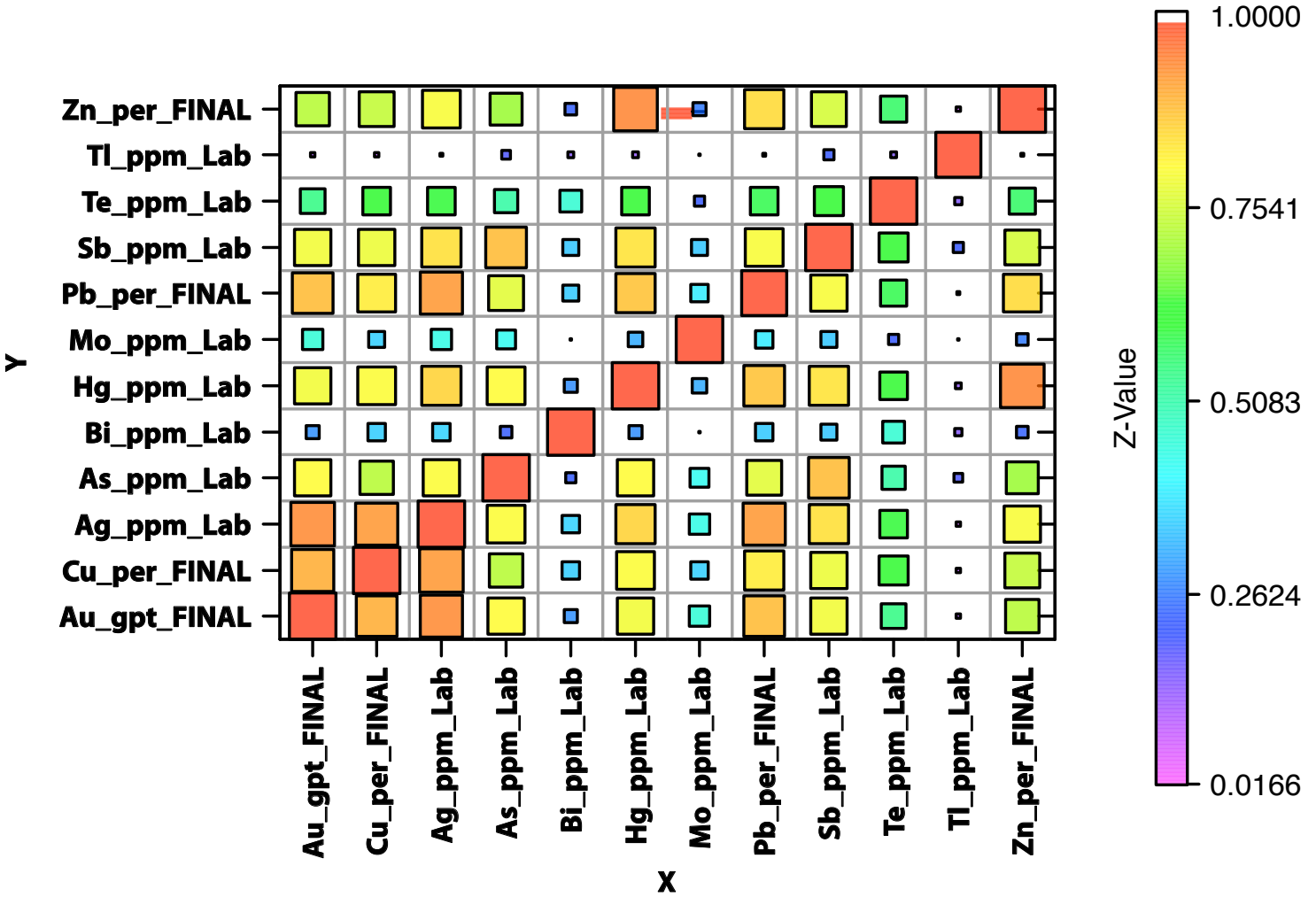

Figure 23. Correlation matrix of assay data from the 1806 zone. Data have been log transformed prior to data manipulation (e.g., Davis, 2002; Grunsky and Kjarsgaard, 2008). Stronger correlations are in hotter colours, weaker correlations are in cooler colours. Notably there are moderate to strong correlations between Au-Ag-enrichment and Cu< As, Hg, Pb, and Sb, elements that are commonly associated with magmatic volatiles, suggesting that the Au-Ag-enrichment in the Rambler deposit is likely due to a magmatic volatile contribution to the Ming VMS system.